Published in final edited form as:
Toxicol Appl Pharmacol. 2009 October 15; 240(2): 273–285. doi:10.1016/j.taap.2009.07.025.

Vanadium Induces Dopaminergic Neurotoxicity Via Protein Kinase C-Delta Dependent Oxidative Signaling Mechanisms: Relevance to Etiopathogenesis of Parkinson's Disease

Hilary Afeseh Ngwa[1], **Arthi Kanthasamy**[1], **Vellareddy Anantharam**[1], **Chunjuan Song**[1], **Travis Witte**[2], **R. S. Houk**[2], and **Anumantha G. Kanthasamy**[1,*]

[1] Department of Biomedical Sciences, Iowa Center for Advanced Neurotoxicology, Iowa State University, Ames, IA 50011, USA

[2] Ames Laboratory, U. S. Department of Energy, Department of Chemistry, Iowa State University, Ames, Iowa 50011 USA

Abstract

Environmental exposure to neurotoxic metals through various sources including exposure to welding fumes has been linked to an increased incidence of Parkinson's disease (PD). Welding fumes contain many different metals including vanadium typically present as particulates containing vanadium pentoxide (V_2O_5). However, possible neurotoxic effects of this metal oxide on dopaminergic neuronal cells are not well studied. In the present study, we characterized vanadium-induced oxidative stress-dependent cellular events in cell culture models of PD. V_2O_5 was neurotoxic to dopaminergic neuronal cells including primary nigral dopaminergic neurons and the EC_{50} was determined to be 37 μM in N27 dopaminergic neuronal cell model. The neurotoxic effect was accompanied by a time-dependent uptake of vanadium and upregulation of metal transporter proteins Tf and DMT1 in N27 cells. Additionally, vanadium resulted in a threefold increase in reactive oxygen species generation, followed by release of mitochondrial cytochrome c into cytoplasm and subsequent activation of caspase-9 (>fourfold) and caspase-3 (>ninefold). Interestingly, vanadium exposure induced proteolytic cleavage of native protein kinase Cdelta (PKCδ, 72-74 kDa) to yield a 41 kDa catalytically active fragment resulting in a persistent increase in PKCδ kinase activity. Co-treatment with pan-caspase inhibitor ZVAD-FMK significantly blocked vanadium-induced PKCδ proteolytic activation, indicating that caspases mediate PKCδ cleavage. Also, co-treatment with Z-VAD-FMK almost completely inhibited V_2O_5-induced DNA fragmentation. Furthermore, PKCδ knockdown using siRNA protected N27 cells from V_2O_5-induced apoptotic cell death. Collectively, these results demonstrate vanadium can exert neurotoxic effects in dopaminergic neuronal cells via caspase-3-dependent PKCδ cleavage, suggesting that metal exposure may promote nigral dopaminergic degeneration.

***Corresponding author:** Dr. Anumantha G. Kanthasamy, Distinguished Professor and Lloyd Chair, Parkinson's Disorder Research Laboratory, Iowa Center for Advanced Neurotoxicology, Department of Biomedical Sciences, 2062 Veterinary Medicine Building, Iowa State University, Ames, IA 50011, Phone: 01-515-294-2516; Fax: 01-515-294-2315; akanthas@iastate.edu.

Keywords

metal mixtures; vanadium; manganese; neurotoxicity; oxidative stress; Parkinson's disease

Introduction

Parkinson's disease (PD) is a multifactorial chronic neurodegenerative disorder associated with progressive degeneration of nigral dopaminergic neurons in the mesencephalic midbrain region resulting in substantial loss of dopaminergic neurotransmission to the striatal region (Anglade et al., 1997). The etiopathogenesis of PD is still poorly understood; however, chronic exposure to certain metals such as manganese (Mn) has been implicated in PD pathogenesis (Dobson et al., 2004). Epidemiological and case-control studies conducted in the United States as well as other countries have linked heavy metal exposure to an increased incidence of PD (Gorell et al., 1997; Fleming, 1994; Schulte, 1996; Liou, 1997; Marder, 1998; Smargiassi, 1998; Taylor, 1999; Priyadarshi, 2000; Tuchsen, 2000; Ritz, 2000). Subtle preclinical neurological effects have recently been documented following exposure to very low levels of Mn in occupational settings (Mergler, 1999; Crossgrove and Zheng, 2004). Since Mn elimination from the central nervous system (CNS) typically occurs very slowly, delayed neurotoxic effects may occur later in life resulting in an increased frequency of Parkinsonian diseases in the geriatric population (Alessio and Lucchini, 1996; Cranmer et al., 1999; Lucchini et al., 1995; Lucchini et al., 1997). Early life exposure to heavy metals such as lead has been shown to produce Alzheimer's-like pathology in rodents as well as in primate models (Wu et al., **2008**). Two studies have shown that welders are at an increased risk for the development of PD (Racette et al., 2001; Park et al., 2005), while another study did not find such an association between welding and a risk for developing Parkinsonism (Goldman et al., 2005; Ellingsen et al., 2008). Welding fumes contain many different metals including manganese, iron, and vanadium, typically present as vanadium pentoxide (V_2O_5). However, the neurotoxic effects of V_2O_5 are not well understood.

Vanadium continues to be widely used in various industrial applications including steelmaking; arc welding; temperature-resistant alloy production; and glass, pigment and paint manufacturing (Hazardous Substance Database, ChemIDPlus, 2006; Bunting, 2006; McNeilly et al., 2004). Vanadium is a preferred metal for the production of special steels and temperature-resistant alloys because it is one of the lightest high-strength metals. More than 90% of industrial vanadium is used in steel making. The dominant market driver for vanadium over the past three years has been an increased worldwide demand for higher strength steel, most notably in China (Bunting, 2006). This increased demand for vanadium is not expected to decline as the worldwide demand for high quality steel continues. Welding and the associated exposure of workers to welding fumes have increased along with steel production. Among nine metals (Co, Cr, Cu, Fe, Mn, Ni, Ti, V and Zn) characterized in welding fumes by use of inductively coupled plasma mass spectroscopy (ICP-MS), vanadium was present at about half the concentration of Mn (McNeilly et al., 2004). The use of vanadium with non-ferrous metals is of particular importance in the atomic energy industry, aircraft construction and space technology (Hazardous Substance Database, ChemIDPlus, 2006). Notably, vanadium compounds are released into the environment in large quantities, mainly by burning fossil fuels. Vanadium is usually found to be the most abundant trace metal in petroleum samples and can be found in concentrations reaching 1500 mg kg^{-1} depending on the source of the crude oil (Amorim et al., 2007). Vanadium accumulates in the soil, groundwater, and plants that may be consumed by animals and humans (Pyrzynska and Weirzbicki, 2004).

Despite these widespread use of vanadium, the health effects of the metal, in particular the CNS effects, are not well characterized. While earlier studies have shown vanadium exposure

in humans may cause CNS deparession, tremor, neurasthesia and other severe motor deficits including vegetative symptoms (WHO, 2000; Done, 1979), the neurotoxic effects of vanadium and its potential to induce chronic neurological diseases are not well understood. Another recent study showed that inhaled V_2O_5 can damage the nigrostriatal dopaminergic system in rodent models (Avila-Costa et al., 2004), but the mechanism of vanadium-induced dopaminergic neurotoxicity is yet to be defined.

Oxidative stress and apoptosis are regarded as key mediators of neurodegenerative processes in PD (Hartmann et al., 2000; Dawson and Dawson, 1996; Olanow et al., 2004; Olanow and Tatton, 1999; Olanow, 2004) and are neurotoxic sequelae resulting from metal exposure (Kanthasamy et al., 2003; Kitazawa et al., 2003; Hamai and Bondy, 2004; Latchoumycandane et al., 2005). Our lab previously reported that increased oxidative stress during exposure to Parkinsonian neurotoxicants, as well as pesticides and metals, can activate the proapoptotic kinase PKCδ by caspase-3-dependent proteolysis in cell culture models of PD (Kitazawa et al., 2003; Kaul et al., 2003, 2005(a), 2005(b); Latchoumycandane et al., 2005). Proteolytic cleavage of PKCδ (74 kDa) by caspase-3 results in a 41 kDa catalytic subunit and a 38 kDa regulatory subunit, leading to a persistent activation of the kinase (Kaul et al., 2003; Kitazawa et al., 2003; Anantharam et al., 2004; Yang et al., 2004). Blockade of proteolytic activation of PKCδ by overexpression of the kinase-dominant negative mutant, cleavage-resistant mutant, or siRNA directed against PKCδ almost completely prevented dopaminergic cell death (Kaul et al., 2003; Kitazawa et al., 2003, 2005; Anantharam et al., 2004; Yang et al., 2004), demonstrating that PKCδ is a key proapoptotic and oxidative stress sensitive kinase in dopaminergic neurons. In the present study, we examined the effect of V_2O_5 on oxidative signaling in a dopaminergic cell model of PD.

Methods

Chemicals

Vanadium pentoxide (V_2O_5) and MTT were purchased from Sigma (St. Louis, MO); Sytox green nucleic dye and COX IV antibody were purchased from Molecular Probes (Eugene, OR). Ac-DEVDAFC (Acetyl-Asp-Glu-Val-Asp-7-amido-4-trifluoromethylcoumarin), Ac-LEHD-AFC (Acetyl-Leu-Glu-His-Asp-7-amido-4-trifluoromethylcoumarin), and Z-VAD-FMK (Z-Val-Ala-Aspfluoromethyl ketone) were purchased from MP Biomedicals (Aurora, OH). Cell Death Detection ELISA plus Assay Kit was purchased from Roche Molecular Biochemicals (Indianapolis, IN). Bradford protein assay kit was purchased from Bio-Rad Laboratories (Hercules, CA). RPMI 1640, B27 supplement, fetal bovine serum, L-glutamine, penicillin, and streptomycin were purchased from Invitrogen (Gaithersburg, MD). Nitric acid was purchased from Fisher Scientific (Pittsburgh, PA). Anti-mouse DMT-1 (1μg/ml) and anti-mouse transferrin (Tf) (1μg/ml) were purchased from Alpha Diagnostic International, San Antonio, TX. Protease cocktail, phosphatase inhibitors, ATP, Protein ASepharose, protein-G-Sepharose and anti-β-actin antibody were obtained from Sigma-Aldrich (St. Louis, MO); rabbit PKCδ antibody was purchased from Santa Cruz Biotechnology, Inc. (Santa Cruz, CA); cytochrome c antibody was purchased from BD Biosciences, anti-mouse and anti-rabbit secondary antibodies (Alexa Flour 680 conjugated anti-mouse IgG and Rabbit IgG IR800 Conjugate) were purchased from Invitrogen and Rockland Inc., respectively. [γ-^{32}P]ATP and ^{3}H-DA were purchased from Perkin Elmer Life Science (Boston, MA).

Cell culture

We used the rat mesencephalic dopaminergic cell line referred to as N27 cells, which was a gift from Dr. Kedar N. Prasad (University of Colorado Health Sciences Center, Denver, CO). N27 cells have been used extensively to study the neurotoxic mechanisms pertaining to Parkinson's disease (Clarkson et al., 1999; Kaul et al., 2003; Kaul et al., 2005a; Kaul et al.,

2005b; Miranda et al., 2004; Peng et al., 2005). N27 cells were grown and treated in RPMI 1640 medium supplemented with 10% fetal bovine serum, 2 mM L-glutamine, 50 units of penicillin, and 50 μg/ml of streptomycin in a humidified atmosphere of 5% CO_2 at 37°C as described previously (Kaul et al., 2003; Yang et al., 2004). For antioxidant studies, N27 cells were treated in RPMI 1640 medium supplemented with 2% B27 supplement with or without antioxidants instead of 10% fetal bovine serum.

We also used mouse fetal primary mesencephalic cultures to determine the effect of vanadium on dopaminergic neurons. We prepared nigral primary mesencephalic neuronal cultures from the ventral mesencephalon of gestational 14-d-old mice embryos as described previously (Yang et al., 2004, Zhang et al., 2007). The mesencephalic tissues from mice were dissected, maintained in ice-cold Ca^{2+}-free HBSS and then dissociated in HBSS solution containing trypsin-EDTA (0.25%) for 20 min at 37°C. The dissociated cells were then plated at equal density (0.5×10^6 cells) in 30-mm-diameter tissue culture wells which had been precoated with poly-D-lysine (1 mg/ml). The primary cultures were maintained in a chemically defined medium consisting of neurobasal medium fortified with B-27 supplements, L-glutamine (500 μM), penicillin (100 IU/ml), and streptomycin (100 μg/ml) (Invitrogen). The cells were maintained in a humidified CO_2 incubator (5% CO_2, 37°C) and half of the culture medium was replaced every 2 d. Approximately 5- to 7-d-old cultures were used for experiments.

Treatment paradigm

For the purpose of this study, vanadium interchangeably refers to vanadium pentoxide (V_2O_5) dissolved in water (moles of V_2O_5/L). N27 cells were treated with different concentrations of vanadium for the duration of the experiments using **diluted stock solution in culture media.** After treatment, cells were collected by trypsinization or scraping, spun down at 200*g* for 5 min, and washed with ice-cold phosphate-buffered saline (PBS). The lysates from the cell pellets were used for various assays including caspase-3 activity, Western blotting, and measurement of DNA fragmentation.

Assessment of cell death by Sytox Green assay

The assessment of cytotoxicity was conducted using Sytox Green, a membrane-impermeable DNA dye that enters dead cells as a result of altered membrane permeability and intercalates into the nucleic acid, as described previously (Kaul et al., 2005; Latchoumycandane et al., 2005). DNA-bound Sytox Green can be detected at an excitation wavelength of 485 nm and an emission wavelength of 538 nm using a fluorescence microplate reader (Bio-Tek microplate reader). The intensity of fluorescence is directly proportional to the number of dead cells; this method is known to be more efficient and sensitive than other cytotoxicity measurements (Kitazawa et al., 2004). Equal numbers of subconfluent N27 cells grown in 24-well plates were co-incubated with 1 μM Sytox Green and with appropriate concentrations of vanadium or RPMI medium as a control. To quantify cell death, fluorescence intensity was monitored after the experiments were conducted and fluorescence pictures were taken using a Nikon inverted fluorescence microscope equipped with a SPOT digital camera (Diagnostic Instruments, Sterling Heights, MI).

3-(4,5-dimethylthiazol-3-yl)-2,5-diphenyl tetrazolium bromide (MTT) assay

This assay has been widely used to assess cell viability by measuring the activity of mitochondrial dehydrogenase enzymes that cleave the tetrazolium ring to produce formazan (Brown et al., 1994; Kitazawa et al., 2001; Choi et al., 2007). After vanadium treatment, cells were washed once and further incubated in serum-free DMEM containing 0.25 mg/ml MTT for 1 h at 37°C. Supernatant was removed, and MTT crystals were solubilized in 200 μl dimethyl sulfoxide. The mitochondrial activity was measured with the SpectraMax

spectrophotometer (Molecular Devices Corporation, San Diego, CA) at 570 nm, with the reference wavelength at 630 nm.

Determination of intracellular vanadium concentration

N27 cells were treated with 40 μM vanadium for 0, 4.5 and 9 h and washed three times with PBS. Inductively coupled plasma mass spectrometry (ICP-MS) was used to determine the concentrations of V at m/z 51 in each sample. The ICP-MS device (ELEMENT 1, Thermo Finnigan) was a high-resolution double focusing instrument operated in medium resolution ($m/\Delta m = 4{,}000$) in order to resolve the isotopes of interest from any interferences (Shum et al., 1992). Each sample was placed in an acid-washed 5 ml Teflon vial and digested in 150 μl high purity nitric acid (Ultrex II, J.T. Baker). Following digestion, the samples were diluted to 5 ml with 18.2 MΩ deionized water to give a final acid concentration of approximately 3% nitric acid. The supernatant was analyzed with the ICP-MS.

An internal standard method was used for quantification. Gallium was chosen as the internal standard because its m/z ratio is similar to that of the elements of interest, and it has no major spectroscopic interferences. A small spike of Ga standard solution was added to each sample for a final Ga concentration of 10 ppb. A 10 ppb multi-element standard (V, Mn, Fe, Cu, Zn, Ga) was prepared. The nitric acid blank, the multi-element standard, and each of the samples were introduced into the ICP-MS via a 100 μl/min self-aspirating PFA nebulizer (Elemental Scientific, Inc.). The nitric acid blank was used to rinse the nebulizer between each sample.

The results for each sample were calculated using the integrated average background-subtracted peak intensities from 20 consecutive scans. To correct for differences in elemental ionization efficiency in the ICP, the multi-element standard was used to derive normalization factors for V, Mn and Cu. Concentrations for V, Mn and Cu were then calculated for each sample.

Determination of vanadium-induced H_2O_2 production by polarography

N27 cells (~ 10,000 per well) were grown in 96 well plates 12-18 h prior to treatments and then exposed to vanadium under serum free conditions for 4 h. H_2O_2 production in N27 cells was measured using an Apollo 4000 Free Radical Analyzer (WPI, Sarasota, FL) equipped with a 100-μm H_2O_2 sensor following a 4 h vanadium exposure. Before the experiment, the electrode was calibrated using serial dilutions of H_2O_2, and the current recorded from the serum free RPMI media over the cells was then calculated as concentration of H_2O_2. The APOLLO 4000 Free-Radical Analyzer (World Precision Instruments, Inc., Sarasota, FL, USA), which is increasingly being used (Mastore et al., 2005; Castello et al., 2007), was used to monitor in real-time the production of H_2O_2 during vanadium treatment. A pulse voltage (+400 mV) maintained on a sensitive and selective H_2O_2 sensor (ISO-HOP2) ensured that the electrochemical responses (redox current) generated at the working electrode were derived only from the oxidation of any H_2O_2 formed, and that these responses were proportional to the concentration of the reactive molecule. Quantitative determinations were made following the establishment of calibration curves for the H_2O_2 electrode prior to all tests. The latter was obtained by plotting changes in current (pA) against changes in H_2O_2 concentration. Test conditions, such as temperature and pH, were identical to those under which the instrument was calibrated (Mastore et al., 2005). To assess H_2O_2 production, the electrode was allowed to equilibrate for 1–3 min in treatment media on cells in the wells of the 96 well plate.

Measurement of caspase-3 and caspase-9

Caspase-3 and caspase-9 activities were measured as previously described in our lab publications (Anantharam et al., 2002; Kaul et al., 2003; Kitazawa et al., 2003; Kitazawa et al., 2002). After exposure to vanadium, the cells were washed with PBS, resuspended in lysis

buffer containing 50 mM Tris/HCl (pH 7.4), 1 mM EDTA, 10 mM EGTA, and 10 μM digitonin, and incubated at 37°C for 20 min. Lysates were centrifuged at 132,000 g, and the cell-free supernatants were incubated with 50 μM Ac-DEVD-AFC (fluorometric caspase-3 substrate) or 50 μM Ac-LEHD-AFC (fluorometric caspase-9 substrate) at 37°C for 1 h. Formation of 7-amido-4-trifluoromethylcoumarin (AFC) resulting from caspase cleavage was measured using a fluorescence plate reader (excitation 400 nm, emission 505 nm). All the fluorescence signals from the samples were normalized to protein concentration, as determined with the Bradford protein assay.

DNA fragmentation assay

DNA fragmentation assays were performed using a Cell Death Detection ELISA plus Assay Kit, which is fast, highly sensitive and reliable for the detection of early changes in cells undergoing apoptotic cell death. The assay analyzed DNA fragmentation by quantification of histone-associated low molecular weight DNA in the cytoplasm of cells (Anantharam et al., 2002; Kaul et al., 2003; Kitazawa et al., 2002). DNA fragmentation was measured in N27 cells exposed to vanadium at time points correlating with maximum caspase-3 activation. In inhibitor studies, pan-caspase inhibitor ZVAD-FMK (100 μM) was co-treated (after a 30 min pretreatment with the inhibitors alone) with 40 μM vanadium for 9 h. After treatment, 20 μl of cell lysate was prepared according to the manufacturer's protocol, as previously described (Choi et al., 2007). Briefly, vanadium-treated cells were washed with PBS, and the cell pellets were then resuspended with the lysis buffer provided in the assay kit. The lysate was spun down at 200*g*, and 20 μl of supernatant was incubated for 2 h with the mixture of HRP-conjugated antibody that recognizes histones and single- and double-stranded DNA. After washing away the unbound components, the final reaction product was measured colorimetrically with 2,2′-azino-di-[3-ethylbenz-thiazoline sulfonate] as an HRP substrate using a spectrophotometer at 405 nm and 490 nm. The difference in absorbance between 405 and 490 nm was used to determine the amount of DNA fragmentation in each sample. All sample concentrations were normalized to protein concentration using the Bradford protein assay.

PKCδ knockdown by siRNA in N27 cells

PKCδ-siRNA was prepared by an *in vitro* transcription method, as described previously (Yang et al., 2004). Initially, siRNA target sites specific to rat PKCδ mRNA (gene identifier: 18959249), as determined by blast analysis, were chosen. One nonspecific siRNA (NS-siRNA) was also chosen based on random sequence. For each siRNA, sense and antisense templates were designed based on each target sequence and partial T7 promoter sequence (Donze and Picard, 2002): for PKCδ-siRNA, sense, 5′-AACTGTTTGTGAATTTGCCTTCCTGT CTC-3′; antisense, 5′-AAAAGGCAAATTCACAAACAGCCTGTCTC-3′ with the target site located at nucleotide 2142 to 2162 in rat PKCδ mRNA with a GC content of 47.6%; for NS-siRNA, sense, 5′-AATTCTCACACTTCGGAGAACCTGTCTC-3′; antisense, 5′-AAGTTCTCCG AAGTGTGAGAACCTGTCTC-3′. All template oligonucleotides were chemically synthesized and PAGE purified. *In vitro* transcription, annealing, and purification of siRNA duplexes were performed using the protocol supplied with the silencer siRNA construction kit (Ambion, Austin, TX). Briefly, ~2 μg of each single-strand (ss) transcription template was first annealed with the T7 promoter and filled in by Klenow DNA polymerase to form double-strand transcription templates. For preparation of each siRNA duplex, transcription reactions were first performed with separated antisense and sense templates using the T7 RNA polymerase provided with the kit and then annealed to form siRNA duplexes. The siRNA duplex was then treated with DNase and RNase to remove the extra nucleotides of transcribed siRNA to meet the structural 3′UU overhang and 5′ phosphate requirement (Elbashir et al., 2001). Previously, we showed that PKCδ-siRNA effectively suppresses >80% of PKCδ protein expression levels within 24 h post-transfection (Yang et al., 2004). N27 cells (50–70% confluence) were

transfected with siRNA duplexes by using an AMAXA Nucleofector kit (AMAXA), as described in our lab's previous study (Yang et al., 2004).

Protein kinase Cδ activity

PKCδ enzymatic activity was determined using immunoprecipitation, as described previously (Kitazawa et al., 2003; Kaul et al., 2005). The cells were exposed to 40 μM vanadium for 9 h, with or without a pan-caspase inhibitor (Z-VAD-FMK), and cell lysates were collected. After immunoprecipitation with anti-PKCδ antibody, 25 μl samples containing PKCδ bound to Sepharose-A beads were incubated with 25 μl of reaction buffer containing 0.4 mg of histone H1 and 5 μCi of [γ-^{32}P]ATP (4500 Ci/mM) for 10 min at 30°C. The reaction was terminated by the addition of 2x SDS gel loading buffer and boiled for 5 min. The samples were separated on 12% SDS-PAGE and histone phosphorylated bands were detected using a PhosphoImager (Personal Molecular Imager FX, Bio-Rad) and quantified using Quantity One 4.2.0 Software (Bio-Rad).

Western blotting

N27 neuronal cells were exposed to 40 μM V_2O_5 with or without the pan-caspase inhibitor (ZVAD-FMK) at 37°C for appropriate time points. N27 cells were lysed, homogenized, sonicated, and centrifuged as described previously (Kaul et al., 2003; Kitazawa et al., 2002). The supernatants were collected as cell lysates, and protein concentrations were determined and used for SDS-gel electrophoresis according to standard procedure. Whole cell lysates and cytoplasmic and mitochondrial fractions, as appropriate, containing equal amounts of protein were loaded in each lane and separated on a 10-15% SDS-PAGE gel, as described previously (Kaul et al., 2003; Kitazawa et al., 2002). Proteins were then transferred to nitrocellulose membrane, and non-specific binding sites were blocked by incubation for 1 h in Licor buffer. The membranes were then treated with the appropriate primary antibodies, PKCδ polyclonal antibody (1:2000), cytochrome c (1:500), COX IV(1:500), Tf (1:500), and DMT1 (1:500) followed by treatment with secondary anti-mouse or anti-rabbit antibodies, as appropriate. To confirm equal protein in each lane, membranes were probed with β-actin antibody (1:5000 dilution). Western blot was performed using IR dye-800 conjugated anti-rabbit dye and Alexa Flour 680 conjugated anti-mouse IgG as secondary antibodies. Western blot images were captured and analyzed with an Odyssey IR Imaging system (LICOR).

Dopaminergic Neuronal Viability by ^{3}H-Dopamine (^{3}H-DA) Uptake Assay

The neurotoxic effect of V_2O_5 on dopaminergic neurons in fetal mouse mesencephalic cultures were quantified using ^{3}H-DA uptake assay described in detail elsewhere (Michel et al., 1990; Vaglini et al., 2008). In our experience, we noted that ^{3}H-DA uptake assay was more robust and quantitative than tyrosine hydroxylase (TH) positive cell counts by immunohistochemical method. Briefly, mouse primary mesencephalic neuronal cultures were treated with 10, 20, 40 or 60 μM V_2O_5 for 12 h and then cells were washed once with assay incubation (Kreb's Ringer) buffer (5.6mM glucose, 1.3mM EDTA, 1.2mM magnesium sulfate, 1.8mM calcium chloride, 4.7mM potassium chloride, 120mM sodium chloride, 16mM sodium phosphate). Cells were incubated with 10μM ^{3}H-DA (30Ci/mol) for 30 min at 37°C. The dopamine reuptake blocker Mazindol (1nM) was used as a positive control to assess the efficiency of ^{3}H-DA uptake. The uptake was stopped by removing the reaction mixture and followed by a three-time wash with fresh Kreb's Ringer buffer. Cells were then collected with 1N sodium hydroxide and the radioactivity was measured by liquid scintillation counter after the addition of a 4mL scintillation cocktail to each vial.

Statistical analysis

Data were analyzed with Prism 3.0 software (GraphPad Software, San Diego, CA). Tukey's multiple comparison testing was used to compare differences between treatment groups of N27 cells. For the cell viability assay, a nonlinear regression curve was fit onto the data, and EC_{50} concentrations were extrapolated (Choi et al., 2007). For comparison between two samples, Student's T-test was performed to examine the differences. Differences with * $p<0.05$, ** $p<0.01$, and *** $p<0.001$ were considered significant and are indicated by asterisks. Presented data typically represent results from at least two separate experiments with triplicate samples where appropriate, and are expressed as mean ± S.E.M.

Results

Vanadium exposure induces dose-dependent increase in cytotoxicity

In order to determine the optimal dose for a detailed mechanistic investigation of vanadium neurotoxicity, we first performed a dose-response cytotoxicity analysis. N27 cells were exposed to 3-300 M vanadium (V_2O_5) for 12 h, and a dose-dependent effect of vanadium on cytotoxic cell death was determined by MTT assay. As shown in Fig. 1A, a dose-dependent decrease in cell viability was observed. An EC_{50} of **37 ± 3.47** μM for vanadium was deduced by three-parameter nonlinear regression from the dose-response curve. The dose-dependent effect of vanadium-induced cell death was further confirmed by Sytox Green fluorescence assay, which labels green only dead/dying cells both qualitatively and quantitatively. N27 cells were exposed to 10-300 μM vanadium for 12 h. Fig. 1B is representative of untreated and vanadium-treated N27 cells at the end of a 12 h treatment in phase-contrast (left panels) and Sytox FITC fluorescence imaging (right panels). An increase in the number of Sytox-positive green cells indicates an increase in cell death because the Sytox Green dye permeates compromised cell membranes to stain nuclear chromatin. The number of Sytox-positive cells increased dose-dependently in vanadium-treated cells compared to untreated controls. Quantitative analysis of Sytox fluorescence using a fluorescence plate reader also revealed that vanadium treatment induced cytotoxic cell death in N27 cells. As shown in Fig. 1C, vanadium increased cell death in a dose-dependent manner. Exposure to 10, 30, 100 and 300 μM vanadium over 12 h resulted in a one to sixfold increase in the number of Sytox-positive cells compared to untreated control cells.

Time-dependent uptake of vanadium in N27 dopaminergic cells

Since vanadium induced cytotoxic cell death in a dose-dependent manner, we measured the amount of vanadium entering the cell over time. Previously, we and others have shown that metal ions, Mn, Fe, Zn, Cu, Co, Cd, Al, and V, can be transported by Tf and divalent metal ion transporter (DMT1) (Aschner and Aschner, 1991; Choi et al., 2007; Erikson et al., 2004). Using ICP-MS, we observed a time-dependent uptake of vanadium (Fig. 2A). Exposure to 40 M vanadium to N27 cells resulted in a 7- and 11-fold increase in intracellular levels of vanadium following exposure for 4.5 and 9 h, **respectively.** In addition, we also observed a significant upregulation of transport proteins Tf (Fig. 2B) and DMT1 (Fig. 2C) over time, suggesting that these transport proteins may play a role in the time-dependent uptake of vanadium by the dopaminergic neurons. We also found vanadium treatment altered concentrations of other essential metals including Mn and Cu in the cells. As shown in Fig 2D, intracellular Mn increased by 1.4-fold at 4.5 h of 40 M V_2O_5 treatment whereas the level decreased by 2.7-fold at longer time V_2O_5 exposure (Fig 2D). The intracellular copper increased by 3- and 3.7-fold at 4.5 h and 9 h, respectively, following V_2O_5 exposure (Fig 2E).

Vanadium induces oxidative stress in N27 mesencephalic neuronal cells

Based on the cytotoxicity data and uptake studies, we chose an optimal dose of 40 μM vanadium (V_2O_5) for all subsequent experiments. Several studies, including ours, have shown that dopaminergic neurotoxicants including MPP+, Mn, dieldrin, and MMT induce oxidative stress, alter mitochondrial function and mediate the release of a number of proapoptotic factors including cytochrome c into the cytosol (Kitazawa et al., 2001; Anantharam et al., 2002; Kaul et al., 2003; Kanthasamy et al., 2005) to initiate the apoptotic cascade. Therefore, we examined whether vanadium exposure induces ROS production in dopaminergic cells. In this experiment, we used a very sensitive APOLLO 4000 Free-Radical Analyzer for measurement of H_2O_2 generation. Fig. 3A shows the standard curve for H_2O_2 with R_2 0.999. N27 cells were exposed to 40 μM vanadium for 4 h and then H_2O_2 levels were measured. As shown in Fig. 3B, vanadium exposure induced a threefold significant increase in H_2O_2 production compared with the control, indicating that vanadium can promote oxidative stress in dopaminergic cells.

Next we examined whether vanadium-induced oxidative stress plays a role in the neurotoxicity of vanadium. An antioxidant cocktail (AO) consisting of vitamin E, glutathione, superoxide dismutase (SOD), and catalase was used in the study. N27 cells were exposed to 40 μM vanadium with or without an AO for 12 h and then cytotoxicity was measured by Sytox green fluorescence assay. Co-treatment with AO almost completely protected vanadium-induced neurotoxicity, as seen in phase-contrast (Fig. 3C right panels) and Sytox green fluorescence imaging (Fig. 3C left panels). Quantitative analysis of Sytox fluorescence revealed that AO treatment blocks the threefold increase in neurotoxicity induced by vanadium. These results demonstrate that vanadium-induced oxidative stress plays a key role in mediating the neurotoxicity in dopaminergic cells.

Vanadium exposure promotes mitochondrial cytochrome c release

Previously we showed that exposure to dopaminergic neurotoxins alters mitochondrial function, which can result in the release of a number of proapoptotic factors, including cytochrome c, into the cytosol to initiate the apoptotic cascade in neuronal cells (Kitazawa et al., 2001; Anantharam et al., 2002; Kaul et al., 2003). In the present study, N27 cells were exposed to 40 μM vanadium for 3 and 6 h and the release of cytochrome c into the cytosol was measured by Western blot analysis using antibodies directed against cytochrome c. As shown in Fig. 4, treatment of N27 cells with 40 μM vanadium for 3 and 6 h resulted in a significant increase in cytosolic cytochrome c compared to untreated controls. The mitochondrial marker COX-IV (15-17 kDa) was used for testing the purity of the cytosolic fractions, and no mitochondrial contamination was noted. Nitrocellulose membranes were reprobed with β-actin antibody to confirm equal protein loading.

Vanadium induces a time-dependent activation of caspase-9 and caspase-3

Cytosolic cytochrome c release has been shown to activate multiple caspases, including caspase-9 and caspase-3 (Dawson and Dawson, 2003; Kanthasamy et al., 2003). Caspase-9 and caspase-3 play an important role in the execution of mitochondrial-dependent apoptotic cell death. Since vanadium increased cytochrome c release, we examined the effect of vanadium on the activities of caspase-9 and caspase-3 in N27 cells. Exposure to 40 μM vanadium induced time-dependent increases in caspase-9 (Fig. 5A) and caspase-3 (Fig. 5B) activities compared to untreated controls. Relative to untreated control cells we observed greater than fourfold and ninefold increases in caspase activities for caspase-9 and caspase-3, respectively. Furthermore, co-treatment with 100 μM Z-VAD-FMK, a pan-caspase inhibitor, significantly blocked 40 μM vanadium-induced caspase-9 (Fig. 5C) and caspase-3 (Fig. 5D) enzymatic activities at a level nearly equal to untreated control levels, demonstrating the specificity of caspase activation during vanadium exposure.

Caspase-3 mediates proteolytic cleavage of PKCδ in vanadium exposed N27 cells

Recently, we demonstrated that PKCδ is a prominent endogenous substrate for caspase-3 in dopaminergic cells undergoing apoptotic cell death (Kikkawa et al., 2002; Brodie and Blumberg, 2003; Kanthasamy et al., 2003). Caspase-3 cleaves PKCδ to yield a 41 kDa catalytically active subunit and a 38 kDa regulatory subunit. Proteolytic cleavage of PKCδ results in the permanent dissociation of the regulatory domain from the catalytic fragment, resulting in persistently active kinase. Previously, we showed that Mn and other dopaminergic toxicants induced proteolytic cleavage of PKCδ, but not of PKCα, β, or γ in an isoform specific and caspase-3 dependent manner (Latchoumycandane et al., 2005). Since vanadium exposure resulted in caspase-3 activation in N27 cells (Fig. 5), we examined the proteolytic cleavage of PKCδ in vanadium-treated N27 cells. A 9 h vanadium treatment induced PKCδ cleavage (Fig. 6A), while no cleavage of PKCδ was observed in untreated control cells. In subsequent experiments, we used the cell-permeable caspase inhibitor Z-VAD-FMK to confirm that PKCδ cleavage is mediated by caspase-3. Co-treatment with 100 μM Z-VAD-FMK almost completely blocked vanadium-induced PKCδ cleavage (Fig. 6A), suggesting that the cleavage is indeed mediated by caspase-3. Nitrocellulose membranes were reprobed with β-actin antibody to confirm equal protein loading.

Vanadium induces increases in PKC kinase activity in a caspase-dependent manner

To determine if the vanadium-induced PKCδ cleavage also leads to an increase in PKCδ enzyme activity, we performed immunoprecipitation kinase assays by examining the ability of immunoprecipitated PKCδ to phosphorylate histone H1 using [^{32}P]ATP. We performed the kinase assay in the absence of lipids to measure the increased kinase activity resulting from the persistently active PKCδ catalytic fragment due to proteolytic cleavage, but not by the activation of full-length PKCδ due to membrane translocation. A 9 h treatment with 40 μM vanadium in N27 dopaminergic cells induced a very significant increase in PKCδ kinase activity compared to the control (Fig. 6B). The vanadium-induced PKCδ kinase activity was significantly attenuated in cells co-treated with 100 μM of the pan-caspase inhibitor Z-VAD-FMK. Exposure to 40 μM vanadium for 9 h resulted in increases of 50% and 10% in PKCδ kinase activity in vanadium- and V_2O_5+ Z-VAD-FMK-treated samples, respectively, when compared to untreated control cells, as revealed by densitometric analysis of phosphorylated histone H1 bands (Fig. 6B). These results suggest that proteolytic cleavage of PKCδ mediated by caspase-9 and -3 increases the kinase activity.

Caspases mediate vanadium-induced apoptotic and cytotoxic cell death in N27 cells

Chromatin condensation and DNA fragmentation are hallmarks of apoptosis during metal neurotoxicity (Kanthasamy et al., 2003; 2005). To understand the functional consequence of activation of ROS production, cytochrome c release, and caspase-9, caspase-3 and PKCδ activation, we tested whether vanadium induces apoptosis by using a quantitative DNA fragmentation ELISA assay. Fig. 7A shows that the vanadium-induced DNA fragmentation in N27 cells is significantly attenuated in cells co-treated with the pan-caspase inhibitor Z-VAD-FMK. Exposure to 40 μM vanadium for 9 h caused a fourfold increase in DNA fragmentation compared to untreated control cells, while co-treatment with 100 μM Z-VAD-FMK blocked vanadium-induced DNA fragmentation by more than 60%. Further, we also show that Z-VAD-FMK suppressed vanadium-induced cytotoxic cell death, as measured by Sytox assay (Fig. 7B). Co-treatment with Z-VAD-FMK very significantly attenuated vanadium-induced increases in the number of Sytox-positive cells at the end of a 9 h treatment, as seen in phase-contrast (right panels) and Sytox FITC fluorescence imaging (left panels). Together, these data suggest that both caspases-9 and -3 contribute to vanadium-induced DNA fragmentation.

Suppression of PKCδ by PKCδ siRNA rescues N27 cells from vanadium-induced apoptotic cell death

To further substantiate the functional role of PKCδ in vanadium-induced apoptotic cell death, we examined the effect of PKCδ siRNA on vanadium-induced DNA fragmentation. Our lab has developed PKCδ siRNAs that specifically suppress PKCδ expression without producing any cytotoxic effect in dopaminergic neurons (Yang et al., 2004). Western blot analysis revealed that the protein levels of PKCδ were significantly suppressed in PKCδ-siRNA-transfected cells, whereas PKCδ expression levels were unaltered in non-specific-siRNA (siRNA-NS) or untreated control cells (Fig. 8A). We have shown in our lab that suppression of PKCδ may regulate upstream caspases via a positive feedback amplification loop resulting in the persistent activation of the protein (Kaul, 2003; Kitazawa, 2003). Vanadium-induced caspase-3 activity was significantly blocked in PKCδ-siRNA transfected N27 cells (Fig. 8B). Importantly, PKCδ-siRNA knockdown almost completely blocked vanadium-induced DNA fragmentation, demonstrating a key proapoptotic function of PKCδ in vanadium-induced dopaminergic cell death.

Vanadium induces neurotoxic responses to primary dopaminergic neurons

To determine if vanadium was toxic to nigral dopaminergic neurons, we exposed mouse primary mesencephalic neuronal cultures to various doses of V_2O_5 for 12 h and then assessed the viability of dopaminergic neurons using ^{3}H-DA assay. Mazindol, a dopamine reuptake inhibitor, was used as positive control for the assay. A 12-h treatment with 10, 20, 40, and 60 μM vanadium in nigral primary neuronal cells induced a dose-dependent decrease in dopamine uptake (Fig. 9), indicative of loss of nigral dopaminergic neurons. Forty and 60 μM V_2O_5 produced a significant dopaminergic neuronal degeneration as compared to untreated control cells following at 12 h exposure. These results indicate that vanadium can induce a neurotoxic effect to dopaminergic neurons at low micromolar concentrations.

Discussion

In this study, for the first time to the best of our knowledge, we demonstrate that vanadium can induce oxidative stress and apoptosis in mesencephalic dopamine-producing neuronal (N27) cells through the activation of a series of oxidative stress mediated specific cell death signaling events, including release of cytochrome c from the mitochondria into the cytosol, activation of caspase-9 and caspase-3, proteolytic cleavage of PKCδ, and nuclear DNA breakdown. Using the pharmacological pan-caspase inhibitor Z-VAD-FMK and siRNA against PKCδ, we established that PKCδ is a key downstream mediator of an oxidative stress-caspase-mediated signaling cascade during vanadium-induced apoptosis in dopaminergic neuronal cells. Our results also show that metal transporter proteins Tf and DMT1 may play a key role in the time-dependent uptake and transport of vanadium in dopaminergic neuronal cells. The results from the primary mesencephalic cultures suggest that vanadium can induce degeneration of nigral dopaminergic neurons at low micromolar concentrations.

Acute exposure to vanadium pentoxide has been shown to have major patho-physiological manifestations on the nervous system in humans (WHO, 2000). Severe chronic exposure in humans produces CNS symptomatology including nervous disturbances and neurasthenic or vegetative symptoms (WHO, 2000). Another report showed that individuals exposed to vanadium manifest some neurological disorders such as tremor and CNS depression (Done, 1979). Despite these data on the potential neurotoxic effect of vanadium in humans, only very limited neurotoxicological studies are available to date. Inhalation of vanadium pentoxide in rodent models produces a time-dependent loss of dendritic spines, necrotic-like cell death and considerable alterations of the hippocampus CA1 neurophile, all of which are associated with spatial memory impairment (Avila-Costa et al., 2006). Within the ependymal epithelium, cilia

loss, cell sloughing and cell layer detachment occur after vanadium pentoxide inhalation in rodents (Avila-Costa et al., 2005). This damage disrupts the permeability of the epithelium and promotes access of inflammatory mediators to the underlying neuronal tissue, causing injury and neuronal death (Avila-Costa et al., 2005). Results from a rat study provide evidence that postnatal vanadium exposure through lactation may have an adverse impact upon the physical and neural development of the offspring and on CNS myelination (Soazo and Graciela, 2007). A decreased number of tyrosine hydroxylase immunoreactive neurons in the substantia nigra pars compacta and loss of dendritic spine in the corpus striatum following exposure to vanadium were recently reported in a rat model (Avila-Costa et al., 2004). In the present study, we show that vanadium is neurotoxic in a dopaminergic neuronal model, with an EC_{50} of 37 ± 3.47 μM. In comparison, the EC_{50} of manganese in the same dopaminergic neuronal model was 345 μM (Latchoumycandane et al., 2005), indicating that vanadium is more toxic than manganese in dopaminergic neuronal cells. Cytotoxicity induced by vanadium compounds has been reported in non-neuronal cells (Cortizo *et al.*, 2000; Sabbioni *et al.*, 1991, 1981), and the toxicity of vanadium compounds increases as the valence increases (Barceloux, 1999).

Tf and DMT-1 are major metal transport proteins in CNS. Tf binds several metals including Fe, Mn, Zn, and Cr as well as Cu, Co, Cd, V, and Al and mediates the transport of these metals (Aschner and Aschner, 1991). Another study showed that Mn and Fe are transported by Tf-dependent and -independent pathways, both involving DMT-1 as the transport protein (Erikson et al., 2004). In this study, we saw increased protein levels of Tf and DMT-1, suggesting that they play a role in the time-dependent uptake of vanadium by the dopaminergic neurons. Our results also suggest that the uptake of vanadium by dopaminergic neurons is accompanied by changes in the concentration of other essential metals such as Mn and Cu. Future studies are needed to clarify the mechanisms of vanadium transport in the dopaminergic system.

We have previously shown that exposure to Mn and Mn-containing MMT leads to ROS generation as well as depolarization of the mitochondrial membrane potential in dopaminergic neuronal cells (Anantharam et al., 2002; Kitazawa et al., 2002). We also reported that dopaminergic neuronal cells are more vulnerable to Mn-induced ROS generation and apoptotic cell death than non-dopaminergic cells (Kitazawa et al., 2002), suggesting an increased sensitivity of dopaminergic neurons to metal neurotoxic insult. The literature suggests that metals in an ROS-rich environment may augment the oxidative insult by forming dopamine-derived highly cytotoxic radicals (Junn and Mouradian, 2001; Kitazawa et al., 2001; Kanthasamy et al., 2002) which may contribute to the enhanced susceptibility of dopaminergic neurons to metal-induced neurotoxicity. Vanadium reportedly produces ROS such as hydroxyl free radicals (Cortizo et al., 2000; Gandara et al., 2005) and superoxide, which are further converted to H_2O_2 (Ding et al., 1994). Excessive ROS generation initiates the peroxidative decomposition of the phospholipids of cellular membranes, leading to the propagation of cellular injury. In the present study, we observed that exposure to vanadium increased the generation of H_2O_2 in N27 dopaminergic cells and that an antioxidant cocktail consisting of vitamin E, catalase, superoxide dismutase (SOD) and glutathione can completely prevent vanadium-induced neurotoxicity. Together, our results suggest that oxidative stress plays a major role in the neurotoxic effect of vanadium in dopaminergic neuronal cells.

ROS has been shown to induce cytochrome c release from the mitochondria to cytosol through opening of the mitochondrial transition pore (Liu et al., 1996; Lee and Wei, 2000), and the released cytochrome c serves as a trigger for activation of the caspase-dependent apoptotic cell death cascade (Kaul et al., 2003; Kanthasamy et al., 2005). We observed an accumulation of cytochrome c in the cytosol of vanadium treated N27 cells within 3 h of metal exposure, suggesting that ROS generation, together with the release of cytochrome c from mitochondria may be early events in the vanadium-induced apoptotic cascade. We and others have shown that the initiator caspase-9 and effector caspase-3 play a critical role in the regulation and

execution of apoptosis in dopaminergic neuronal cells (Anantharam et al., 2001; Kaul et al., 2003; Kanthasamy et al., 2003; Cassarino et al., 1999; Dodel et al., 1999). We observed that vanadium exposure dramatically increased both caspase-9 and caspase-3 in a time-dependent manner. Importantly, the caspase inhibitor Z-VAD-FMK significantly protected against vanadium-induced cell death, emphasizing the critical role of caspase activation in this cell death pathway. In terms of PD pathogenesis, caspase-3 activation is a key contributor to apoptosis in dopaminergic neurons in human PD patients as well as in animal models of PD (Hartmann et al., 2000).

Our lab previously established that proteolytic activation of PKCδ by caspase-3 is an important event in the apoptotic cell death of dopaminergic cells following neurotoxic insults (Kanthasamy et al., 2003; Kanthasamy et al., 2005; Kaul et al., 2005). We showed that Mn treatment induces caspase-3-dependent proteolytic cleavage of PKCδ but not of other isoforms, including PKCα or PKCβ, suggesting that the cleavage is isoform-specific (Latchoumycandane et al., 2005). In this study, we showed that vanadium treatment resulted in PKCδ proteolytic cleavage and kinase activation. Co-treatment with the caspase inhibitor Z-VAD-FMK significantly blocked vanadium-induced PKCδ proteolytic cleavage as well as the kinase activity, demonstrating caspase-3 dependent PKCδ activation during vanadium exposure in dopaminergic neuronal cells. The caspase inhibitor also blocked vanadium-induced DNA fragmentation, indicating a role for a caspase-dependent apoptotic cascade in vanadium-induced apoptosis. Furthermore, the knockdown of PKCδ by siRNA completely suppressed vanadium-induced DNA fragmentation, suggesting that PKCδ has a proapoptotic function in vanadium-induced dopaminergic neurotoxicity. The events downstream of PKCδ activation that lead to apoptotic cell death are still unclear. We recently showed that PKCδ translocates to the mitochondria and nucleus following proteolytic activation of the kinase (Sun et al., 2007; 2009). Mn has been reported to inhibit dopamine uptake in striatal synaptosomes (Chen et al., 2006) suggesting that Mn may affect the presynaptic dopaminergic neuronal terminal. We also further showed that vanadium inhibits in a dose-dependent manner the uptake of dopamine in nigral primary neurons indicating that vanadium may also be neurotoxic to dopaminergic neurons in primary nigral cultures. Future studies will focus on identifying key downstream signaling molecules in vanadium-induced dopaminergic degeneration using both cell culture and animal models.

In conclusion, this study demonstrates for the first time that exposure to vanadium induces dopaminergic degeneration by a novel apoptotic pathway mediated by caspase-3-dependent proteolytic activation of PKCδ (Fig. 10). Our current study not only establishes caspase-mediated PKCδ cleavage as a key downstream event of vanadium-induced apoptosis but also emphasizes that blocking ROS, blocking caspase activity and selective targeting of the proapoptotic kinase PKCδ by siRNA can rescue dopaminergic neurons from vanadium-induced dopaminergic degeneration. These findings support the hypothesis that environmental exposure to metals may play an important role in the etiopathogenesis of Parkinsons disease. To further strengthen these findings, a systematic analysis of the vanadium neurotoxic response in the nigrostriatal dopaminergic system in animal models of vanadium neurotoxicity is still warranted.

Acknowledgement

This work was supported by National Institutes of Health (NIH) Grants ES10586 and NS 38644. The W. Eugene and Linda Lloyd Endowed Chair to AGK also is acknowledged. The ICP-MS device was provided by the U. S. Department of Energy, Nuclear Nonproliferation and Basic Energy Sciences Programs. Ames Laboratory is operated under Contract DE-AC02-07CH11358. The authors acknowledge Ms. MaryAnn deVries for her assistance in the preparation of this manuscript.

References

Alessio, L.; Lucchini, R. Data profiles for selected chemicl series. Argentesi, F.; Roi, R.; Sevilla, Marcos JM., editors. European Commission Joint Research Project Centre; Luxembourg: 1996. SPI 96, 59

Amorim FAC, Welz B, Costa ACS, Lepri FG, Vale M, Goreti R, Ferreira SLC. Determination of vanadium in petroleum and petroleum products using atomic spectrometric techniques Talanta 2007;72:349–359.

Anantharam V, Kitazawa M, Wagner J, Kaul S, Kanthasamy AG. Caspase- 3-dependent proteolytic cleavage of protein kinase Cdelta is essential for oxidative stress-mediated dopaminergic cell death after exposure to methylcyclopentadienyl manganese tricarbonyl. J Neurosci 2002;22:1738–51. [PubMed: 11880503]

Anantharam V, Kitazawa M, Latchoumycandane C, Kanthasamy A, Kanthasamy AG. Blockade of PKCdelta proteolytic activation by loss of function mutants rescues mesencephalic dopaminergic neurons from methylcyclopentadienyl manganese tricarbonyl (MMT)-induced apoptotic cell death. Ann NY Acad Sci 2004;1035:271–289. [PubMed: 15681813]

Andersen JK. Oxidative stress in neurodegeneration: cause or consequence. Nature Rev 2004:S18–23.

Anglade P, Vyas S, Javoy-Agid F, Herrero MT, Michel PP, Marquez J, Mouatt-Prigent A, Ruberg M, Hirsch EC, Agid Y. Apoptosis and autophagy in nigral neurons of patients with Parkinson's disease. Histol Histopathol 1997;12:25–31. [PubMed: 9046040]

Aschner M, Aschner J. Manganese neurotoxicity: Cellular effects and blood-brain barrier transport. Neurosci. Biobehav. Rev 1991;15:333–340. [PubMed: 1956602]

Avila-Costa MR, Montiel Flores. E. Colín-Barenque L, Ordoñez JL, Gutiérrez AL, NiñoCabrera G, Mussali-Galante P, Fortoul TI. Nigrostriatal modifi cations after vanadium inhalation: An immunocytochemical and cytological approach. Neurochem Res 2004;29:1365–9. [PubMed: 15202766]

Avila-Costa MR, Fortoul TI, Niño-Cabrera G, Colín-Barenque L, Bizarro- Nevares P, Gutiérrez-Valdez AL, Ordóñez-Librado JL, Rodríguez-Lara V, Mussali-Galante P, Díaz-Bech P, Anaya-Martínez V. Hippocampal cell alterations induced by the inhalation of vanadium pentoxide promote memory deterioration. Neurotoxicology 2006;27:1007–12. [PubMed: 16684564]

Avila-Costa MR, Colín-Barenque L, Zepeda-Rodríquez A, Antuna SB, Saldivar OL, Espejel-Maya G, Mussali-Galante P, Avila-Casado MC, Reyes-Olivera A, Anaya-Martinez V, Fortoul TI. Ependymal epithelium disruption after vanadium pentoxide inhalation. A mice experimental model. Neurosci Lett 2005;381:21–5. [PubMed: 15882783]

Barceloux DG. Vanadium. J. Toxicol. Clin. Toxicol 1999;37:265–278. [PubMed: 10382561]

Brodie C, Blumberg PM. Regulation of cell apoptosis by protein kinase c delta. Apoptosis 2003;8:19–27. [PubMed: 12510148]

Brown DR, Herms J, Kretzschmar HA. Mouse cortical cells lacking cellular PrP survive in culture with a neurotoxic PrP fragment. Neuroreport 1994;5:2057–60. [PubMed: 7865744]

Bunting, Robert M. Vanadium: How market developments affect the titanium industry. Strategic minerals corporation. Titanium; International Titanium Association Conference; San Diego, California. October 3, 2006; 2006.

Cantuti-Castelvetri I, Shukitt-Hale B, Joseph JA. Dopamine neurotoxicity: age-dependent behavioral and histological effects. Neurobiol Aging 2003;24:697–706. [PubMed: 12885577]

Cassarino DS, Parks JK, Parker WD Jr, Bennett JP Jr. The parkinsonian neurotoxin MPP+ opens the mitochondrial permeability transition pore and releases cytochrome c in isolated mitochondria via an oxidative mechanism. Biochim Biophys Acta 1999;1453:49–62. [PubMed: 9989245]

Castello PR, Drechsel DA, Patel M. Mitochondria are a major source of paraquat-induced reactive oxygen species production in the brain. J Biol Chem 2007;282:14186–14193. [PubMed: 17389593]

Chen MK, Lee JS, McGlothan JL, Furukawa E, Adams RJ, Alexander M, Wong DF, Guilarte TR. Acute manganese administration alters dopamine transporter levels in the non-human primate striatum. Neurotoxicology 2006;27:229–236. [PubMed: 16325911]

Choi CJ, Anantharam V, Saetveit NJ, Houk RS, Kanthasamy A, Kanthasamy AG. Normal cellular prion protein protects against manganese-induced oxidative stress and apoptotic cell death. Toxicol Sci 2007;98:495–509. [PubMed: 17483122]

Chun HS, Lee H, Son JH. Manganese induces endoplasmic reticulum (ER) stress and activates multiple caspases in nigral dopaminergic neuronal cells, SN4741. Neurosci Lett 2001;316:5–8. [PubMed: 11720765]

Cranmer J, Mergler D, Williams-Johnson M. Manganese. Are there effects from long-term, low-level exposure ? Neurotoxicology 1999;20:2–3.

Crossgrove JS, Zheng W. Manganese toxicity upon overexposure. NMR in Biomedicine 2004;17:544–553. [PubMed: 15617053]

Cortizo AM, Bruzzone L, Molinuevo S, Etcheverry SB. A possible role of oxidative stress in the vanadium-induced cytotoxicity in the MC3T3E1 osteoblast and UMR106 osteosarcoma cell lines. Toxicology 2000;147:89–99. [PubMed: 10874156]

Dauer W, Przedborski S. Parkinson's disease: mechanisms and models. Neuron 2003;39:889–909. [PubMed: 12971891]

Dawson VL, Dawson TM. Nitric oxide neurotoxicity. J. Chem. Neuroanat 1996;10:179–190. [PubMed: 8811421]

Dawson TM, Dawson VL. Molecular pathways of neurodegeneration in Parkinson's disease. Science (Wash DC) 2003;302:819–822.

Ding M, Gannett PM, Rojanasakul Y, Liu KJ, Shi XL. One-electron reduction of vanadate by ascorbate and related free-radical generation at physiological pH. J. Inorg. Biochem 1994;55:101–112. [PubMed: 8051539]

Dodel RC, Du Y, Bales KR, Ling Z, Carvey PM, Paul SM. Caspase-3-like proteases and 6-hydroxydopamine induced neuronal cell death. Brain Res Mol Brain Res 1999;64:141–148. [PubMed: 9889353]

Done AK. Of metals and chelation. Emer Med 1979;11:186–218.

Donze O, Picard D. RNA interference in mammalian cells using siRNAs synthesized with T7 RNA polymerase. Nucleic Acids Res 2002;30:e46. [PubMed: 12000851]

Elbashir SM, Lendeckel W, Tuschl T. RNA interference is mediated by 21- and 22-nucleotide RNAs. Genes Dev 2001;15:188–200. [PubMed: 11157775]

Ellingsen DG, Konstantinov R, Bast-Pettersen R, Merkurjeva L, Chashchin M, Thomassen Y, Chashchin V. A neurobehavioral study of current and former welders exposed to manganese. Neurotoxicology 2008;29:48–59. [PubMed: 17942157]

Erikson KM, Syversen T, Steinnes E, Aschner M. Globus pallidus: A target brain region for divalent metal accumulation associated with dietary iron deficiency. J. Nutr. Biochem 2004;15:335–341. [PubMed: 15157939]

Fleming L, Mann JB, Bean J, Briggle T, Sanchez-Ramos JR. Parkinson's disease and brain levels of organochlorine pesticides. Ann Neurol 1994;36:100–103. [PubMed: 7517654]

Gandara RMC, Soares SS, Martins H, Gutierrez-Merino C, Aureliano M. Vanadate oligomers: In vivo effects in hepatic vanadium accumulation and stress markers. J Inorg Biochem 2005;99:1238–44. [PubMed: 15833347]

Ghayur T, Hugunin M, Talanian RV, Ratnofsky S, Quinlan C, Emoto Y, Pandey P, Datta R, Huang Y, Kharbanda S, Allen H, Kamen R, Wong W, Kufe D. Proteolytic activation of protein kinase C δ by an ICE/CED 3-like protease induces characteristics of apoptosis. J. Exp. Med 1996;184:2399–2404. [PubMed: 8976194]

Goldman SM, Tanner CM, Olanow CW, Watts RL, Field RD, Langston JW. Occupation and parkinsonism in three movement disorders clinics. Neurology 2005;65:1430–1435. [PubMed: 16162857]

Gorell JM, Johnson CC, Rybicki BA, Peterson EL, Kortsha GX, Brown GG, Richardson RJ. Occupational exposures to metals as risk factors for Parkinson's disease. Neurology 1997;48:650–658. [PubMed: 9065542]

Hamai D, Bondy SC. Pro- or anti-oxidant manganese: a suggested mechanism for reconciliation. Neurochem. Int 2004;44:223–229. [PubMed: 14602085]

Hartmann A, Hunot S, Michel PP, Muriel MP, Vyas S, Faucheux BA, Mouatt-Prigent A, Turmel H, Srinivasan A, Ruberg M, Evan GI, Agid Y, Hirsch EC. Caspase-3: a vulnerability factor and final effector in apoptotic death of dopaminergic neurons in Parkinson's disease. Proc Natl Acad Sci USA 2000;97:2875–2880. [PubMed: 10688892]

Hazardous Substance Database, ChemIDPlus.. 2006.

Hirata Y. Manganese-induced apoptosis in PC12 cells. Neurotoxicol Teratol 2002;24:639. [PubMed: 12200195]

Junn E, Mouradian MM. Apoptotic signaling in dopamine-induced cell death: the role of oxidative stress, p38 mitogen-activated protein kinase, cytochrome c and caspases. J Neurochem 2001;78:374–383. [PubMed: 11461973]

Kanthasamy, AG.; Sharma, N.; Kirby, ML.; Schwarzschild, MA. Neuroprotection: Basic & Clinical Aspects. Prominent Press; 2002. Neuroprotective strategies in Parkinson's disease; p. 604-640.

Kanthasamy AG, Kitazawa M, Kanthasamy A, Anantharam V. Role of proteolytic activation of protein kinase C delta (PKCδ) in oxidative stress-induced apoptosis. Antioxid. Redox Signal 2003;5:609–620. [PubMed: 14580317]

Kanthasamy AG, Kitazawa M, Kanthasamy A, Anantharam V. Dieldrin-Induced Neurotoxicity: Relevance to Parkinson's Disease Pathogenesis. Neurotoxicology 2005;26:701–19. [PubMed: 16112328]

Kaul S, Kanthasamy A, Kitazawa M, Anantharam V, Kanthasamy AG. Caspase-3 dependent proteolytic activation of protein kinase C delta mediates and regulates 1-methyl-4-phenylpyridinium (MPP+)-induced apoptotic cell death in dopaminergic cells: relevance to oxidative stress in dopaminergic degeneration. Eur J Neurosci 2003;18:1387–401. [PubMed: 14511319]

Kaul S, Anantharam V, Kanthasamy A, Kanthasamy AG. Wild-type alpha-synuclein interacts with pro-apoptotic proteins PKCdelta and BAD to protect dopaminergic neuronal cells against MPP+-induced apoptotic cell death. Brain Res Mol Brain Res 2005a;139:137–152. [PubMed: 15978696]

Kaul S, Anantharam V, Yang Y, Choi CJ, Kanthasamy A, Kanthasamy AG. Tyrosine phosphorylation regulates the proteolytic activation of protein kinase Cdelta in dopaminergic neuronal cells. J Biol Chem 2005b;280:28721–30. [PubMed: 15961393]

Kikkawa U, Matsuzaki H, Yamamoto T. Protein kinase Cdelta (PKC-delta): activation mechanisms and functions. J Biochem 2002;132:831–839. [PubMed: 12473183]

Kitazawa M, Anantharam V, Kanthasamy AG. Dieldrin-induced oxidative stress and neurochemical changes contribute to apoptopic cell death in dopaminergic cells. Free Radic Biol Med 2001;31:1473–85. [PubMed: 11728820]

Kitazawa M, Wagner JR, Kirby ML, Anantharam V, Kanthasamy AG. Oxidative stress and mitochondrial-mediated apoptosis in dopaminergic cells exposed to methylcyclopentadienyl manganese tricarbonyl. J Pharmacol Exp Ther 2002;302:26–35. [PubMed: 12065696]

Kitazawa M, Anantharam V, Kanthasamy AG. Dieldrin induces apoptosis by promoting caspase-3-dependent proteolytic cleavage of protein kinase Cdelta in dopaminergic cells: relevance to oxidative stress and dopaminergic degeneration. Neuroscience 2003;119:945–64. [PubMed: 12831855]

Latchoumycandane C, Anantharam V, Kitazawa M, Yang Y, Kanthasamy A, Kanthasamy AG. Protein kinase Cδ is a key downstream mediator of manganese-induced apoptosis in dopaminergic neuronal cells. J Pharmacol Exp Ther 2005;313:46–55. [PubMed: 15608081]

Lee HC, Wei YH. Mitochondrial role in life and death of the cell. J Biomed Sci 2000;7:2–15. [PubMed: 10644884]

Leist M, Volbracht C, Fava E, Nicotera P. 1-Methyl-4-phenylpyridinium induces autocrine excitotoxicity, protease activation, and neuronal apoptosis. Mol Pharmacol 1998;54:789–801. [PubMed: 9804614]

Li L, Lorenzo PS, Bogi K, Blumberg PM, Yuspa SH. Protein kinase Cdelta targets mitochondria, alters mitochondrial membrane potential, and induces apoptosis in normal and neoplastic keratinocytes when overexpressed by an adenoviral vector. Mol Cell Biol 1999;19:8547–8558. [PubMed: 10567579]

Liou HH, Tsai MC, Chen CJ, Jeng JS, Chang YC, Chen SY, Chen RC. Environmental risk factors and Parkinson's disease: a case-control study in Taiwan. Neurology 1997;48:1583–1588. [PubMed: 9191770]

Lucchini R, Selis L, Folli D, Apostoli P, Mutti A, Vanoni O, Iregren A, Alessio L. Neurobeha- vioral effects of manganese in workers from a ferroalloy plant after temporary cessation of exposure. Scand. J. Work. Environ. Health 1995;21:143–149. [PubMed: 7618060]

Lucchini R, Bergamaschi E, Smargiassi A, Apostoli P. Motor function, olfactory threshold and haematological indices in manganese exposed ferroalloy workers. Environmental Research 1997;73:175–180. [PubMed: 9311544]

Marder K, Logroscino G, Alfaro B, Mejia H, Halim A, Louis E, Cote L, Mayeux R. Environmental risk factors for Parkinson's disease in an urban multiethnic community. Neurology 1998;50:279–281. [PubMed: 9443493]

Majumder PK, Mishra NC, Sun X, Bharti A, Kharbanda S, Saxena S, Kufe D. Targeting of protein kinase Cδ to mitochondria in the oxidative stress response. Cell Growth Differ 2001;129:465–470. [PubMed: 11571229]

Mastore M, Kohler L, Nappi AJ. Production and utilization of hydrogen peroxide associated with melanogenesis and tyrosinase-mediated oxidations of DOPA and dopamine. FEBS J 2005;272:2407–2415. [PubMed: 15885091]

McNeilly JD, Heal MR, Beverland IJ, Howe A, Gibson MD, Hibbs LR, MacNee W, Donaldson K. Soluble transition metals cause the pro-inflammatory effects of welding fumes in vitro. Toxicol Appl Pharmacol 2004;196:95–107. [PubMed: 15050411]

Mergler D. Neurotoxic effects of low level exposure to manganese in human populations. Environ Res 1999;80:99–102. [PubMed: 10092399]

Michel PP, Hefti F. Toxicity of 6-hydroxydopamine and dopamine for dopaminergic neurons in culture. J Neurosci Res 1990;26:428–435. [PubMed: 1977925]

Olanow CW. Manganese-Induced parkinsonism and Parkinson's Disease. Ann. N.Y. Acad. Sci 2004;1012:1–15. [PubMed: 15105251]

Olanow CW, Good PF, Shinotoh H, Hewitt KA, Vingerhoets F, Snow BJ, Beal MF, Calne DB, Perl DP. Manganese intoxication in the rhesus monkey: a clinical, imaging, pathologic, and biochemical study. Neurology 1996;46:492–8. [PubMed: 8614520]

Olanow CW, Tatton WG. Etiology and pathogenesis of Parkinson's disease. Annu Rev Neurosci 1999;22:123–44. [PubMed: 10202534]

Park RM, Schulte PA, Bowman JD, Walker JT, Bondy SC, Yost MG, Touchstone JA, Dosemeci M. Potential occupational risks for neurodegenerative diseases. Am J Ind Med 2005;48:63–77. [PubMed: 15940722]

Priyadarshi A, Khuder SA, Schaub EA, Shrivastava S. A meta-analysis of Parkinson's disease and exposure to pesticides. Neurotoxicology 2000;21:435–440. [PubMed: 11022853]

Pyrzynska K, Weirzbicki T. Determination of vanadium species in environmental samples. Talanta 2004;64:823–829. [PubMed: 18969676]

Racette BA, McGee-Minnich L, Moerlein SM, Mink JW, Videen TO, Perlmutter JS. Welding-related parkinsonism: clinical features, treatment, and pathophysiology. Neurology 2001;56:8–13. [PubMed: 11148228]

Ritz B, Yu F. Parkinson's disease mortality and pesticide exposure in California 1984- 1994. Int J Epidemiol 2000;29:323–329. [PubMed: 10817132]

Sabbioni E, Marafante E, Rade J, Gregotti C, Di Nucci A, Manzo L. Biliary excretion of vanadium in rats. Toxicol. Eur. Res 1981;3:93–98. [PubMed: 7245191]

Sabbioni E, Pozzi G, Pintar A, Cassella L, Garattini S. Cellular retention cytotoxicity and morphological transformation by vanadium(IV) and vanadium(V) in BALB/3T3 cell lines. Carcinogenesis 1991;12:47–52. [PubMed: 1988181]

Schwarz A, Burwinkel M, Riemer C, Schultz J, Baier M. Unchanged Scrapie Pathology in Brain Tissue of Tyrosine Kinase Fyn-Deficient Mice. Neurodegenerative Dis 2004;1:266–268.

Schrantz N, Blanchard DA, Mitenne F, Auffredou MT, Vazquez A, Leca G. Manganese induces apoptosis of human B cells: caspase-dependent cell death blocked by bcl-2. Cell Death Differ 1999;6:445–453. [PubMed: 10381635]

Schulte PA, Burnett CA, Boeniger MF, Johnson J. Neurodegenerative diseases: occupational occurrence and potential risk factors, 1982 through 1991. Am J Public Health 1996;86:1281–1288. [PubMed: 8806381]

Shum SC, Neddersen R, Houk RS. Elemental speciation by liquid chromatography-inductively coupled plasma mass spectrometry with direct injection nebulization. Analyst 1992;117:577–82. [PubMed: 1580404]

Smargiassi A, Mutti A, De Rosa A, De Palma G, Negrotti A, Calzetti S. A case-control study of occupational and environmental risk factors for Parkinson's disease in the Emilia-Romagna region of Italy. Neurotoxicology 1998;19:709–712. [PubMed: 9745932]

Soazo M, Garcia GB. “Vanadium exposure through lactation produces behavioral alterations and CNS myelin deficit in neonatal rats”. Neurotoxicology and Teratology 2007;29:503–510. [PubMed: 17493788]

Sun F, Kanthasamy A, Anantharam V, Kanthasamy AG. Environmental neurotoxic chemicals-induced ubiquitin proteasome system dysfunction in the pathogenesis and progression of Parkinson's disease. Pharmacology and Therapeutics 2007;114:327–344. [PubMed: 17521740]

Sun F, Kanthasamy A, Anantharam V, Kanthasamy AG. Mitochondrial accumulation of polyubiquitinated proteins and differential regulation of apoptosis by polyubiquitination sites Lys-48 and -63. J Cell Mol Med. 20092009 – published online

Taylor CA, Saint-Hilaire MH, Cupples LA, Thomas CA, Burchard AE, Feldman RG, Myers RH. Environmental, medical, and family history risk factors for Parkinson's disease: a New England-based case control study. Am J Med Genet 1999;88:742–749. [PubMed: 10581500]

Tuchsen F, Jensen AA. Agricultural work and the risk of Parkinson's disease in Denmark, 1981- 1993. Scand J Work Environ Health 2000;26:359–362. [PubMed: 10994803]

Vega IE, Cui L, Propst JA, Hutton ML, Lee G, Yen SH. Increase in tau tyrosine phosphorylation correlates with the formation of tau aggregates. Brain Res Mol Brain Res 2005;138:135–44. [PubMed: 15913839]

Vaglini F, Pardini C, Viaggi C, Caramelli A, Corsini GU. Apomorphine offers new insight into dopaminergic neuron vulnerability in mesencephalic cultures. Neuropharmacology 2008;55:737–742. [PubMed: 18634808]

WHO. Vanadium. WHO Regional Offi ce for Europe; Copenhagen: Denmark: 2000. p. 9Chapter 6.12

Wu J, Riyaz Basha Md. Brock B, Cox David P. Cardozo-Pelaez F, McPherson CA, Harry J, Rice DC, Maloney B, Chen D, Lahiri DK, Zawia NH. Alteration of Alzheimer disease (AD)-like pathology in aged monkeys after infantile exposure to environmental lead (Pb): Evidence for a developmental origin and environmental link for AD. J. Neurosci 2008;28:3–9. [PubMed: 18171917]

Yang Y, Kaul S, Zhang D, Anantharam V, Kanthasamy AG. Suppression of caspase-3-dependent proteolytic activation of protein kinase C delta by small interfering RNA prevents MPP+-induced dopaminergic degeneration. Mol Cell Neurosci 2004;25:406–421. [PubMed: 15033169]

Zhang D, Anantharam V, Kanthasamy A, Kanthasamy AG. Neuroprotective Effect of Protein Kinase Cδ Inhibitor Rottlerin in Cell Culture and Animal Models of Parkinson's Disease. J Pharmacol Exp Ther 2007;322:913–922. [PubMed: 17565007]

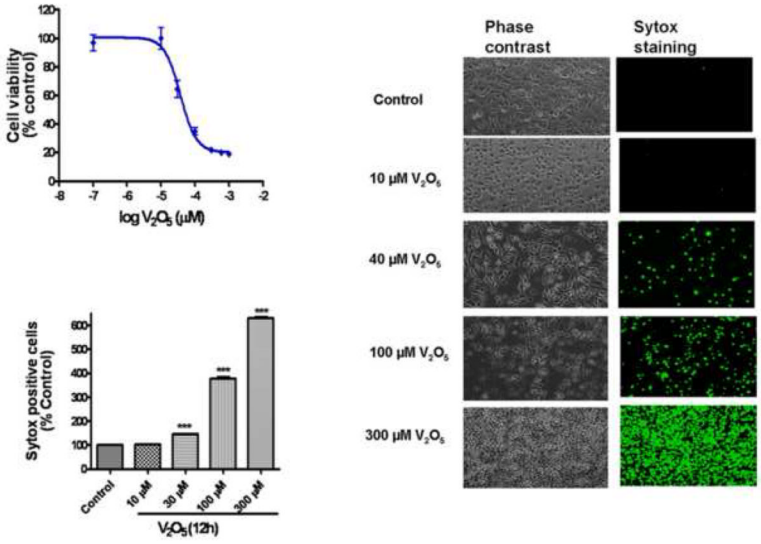

Fig. 1.

Vanadium induces a dose-dependent neurotoxic effect on N27 dopaminergic neuronal cells. **(A)** Effect of vanadium on cell viability in N27 dopaminergic neuronal cells. The cells were exposed to 0-300 μM V_2O_5 and then cell viability was measured using the MTT assay. The value of vanadium neurotoxicity in N27 dopaminergic cells was EC_{50} = 37 ± 3.47 μM. Data represent results from at least eight individual measurements. **(B)** Visualization of vanadium-induced neurotoxicity by Sytox green fluorescence assay. N27 dopaminergic neuronal cells were exposed to 40 μM V_2O_5 for 12 h and then cells were loaded with Sytox green and observed under a Nikon inverted fluorescence microscope and pictures were captured with a SPOT digital camera (Diagnostic Instruments, Sterling Heights, MI). **(C)** Quantitative analysis of vanadium-induced neurotoxicity was measured by the Sytox green cytotoxicity fluorescence assay. The Sytox fluorescence was measured by Bio-Tek fluorescence microplate reader. Data represent results from at least eight individual measurements and are expressed as mean ± S.E.M. The values are expressed as a percentage of untreated control cells. **p<0.001 indicates significant difference with each of the other groups.

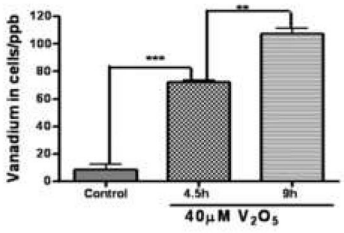

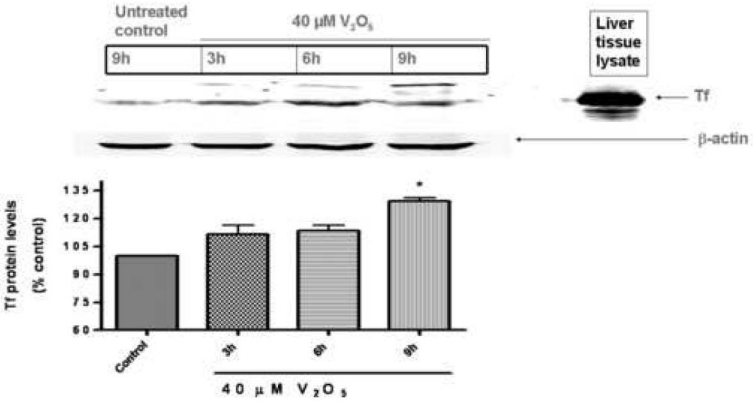

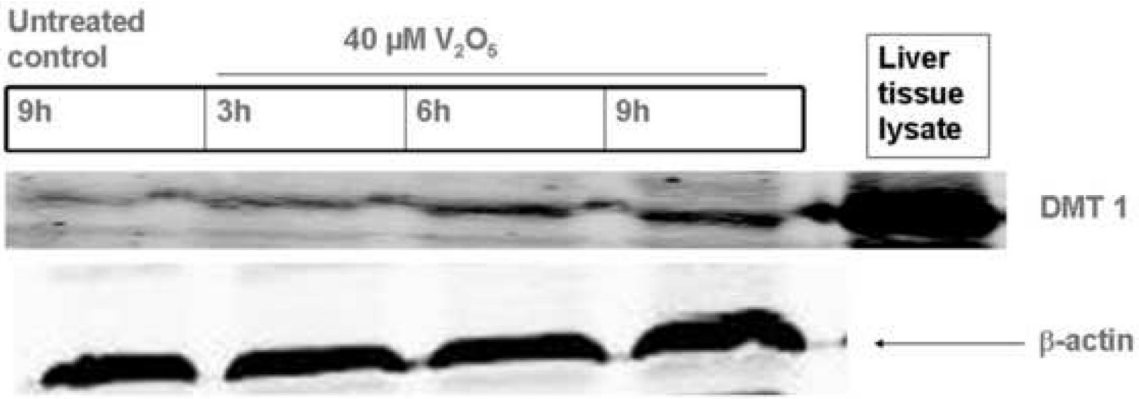

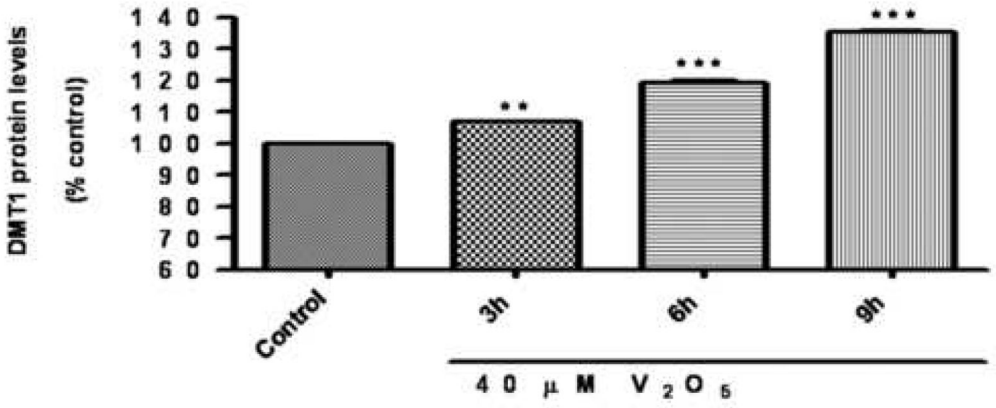

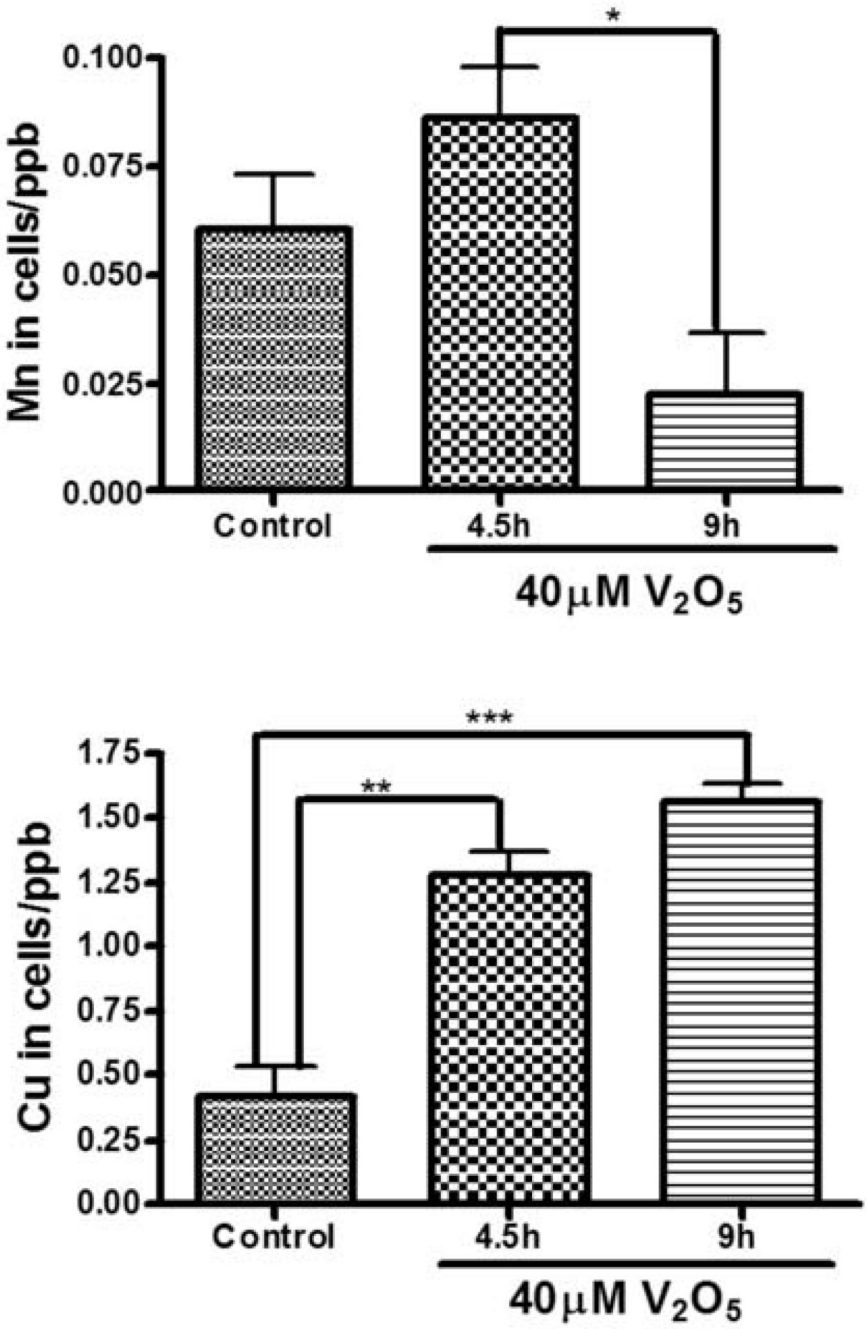

Fig. 2.

Intracellular vanadium uptake and upregulation of metal transport proteins following vanadium exposure in N27 dopaminergic neuronal cells. **(A)** Vanadium uptake in N27 dopaminergic neuronal cells. N27 dopaminergic neuronal cells were exposed to 40 μM vanadium for 4.5 and 9 h and the vanadium content of the cells was measured using the ICP-MS technique. Data represent results from three individual measurements and are expressed as mean ± S.E.M. **p<0.01 and ***p<0.001. Upregulation of Tf **(B)** and DMT1 **(C)**. N27 cells were treated with 40 μM vanadium for 3, 6, and 9 h and then DMT and Tf immunoblot was performed as described in the Methods. To confirm equal protein loading in each lane, the membranes were reprobed with β-actin antibody. Mouse liver lysates were used as a positive control. Data

represent results from at least two separate experiments. Mouse liver lysates were used as a positive control. Data represent results from at least two separate measurements. Data represent results from at least two individual measurements and are expressed as mean ± S.E.M. *p<0.05, **p<0.01 and ***p<0.001 indicates significant difference with control. Vanadium uptake alters intracellular manganese (Mn) concentration (D) and intracellular copper (Cu) concentration (E) in N27 dopaminergic neuronal cells. N27 dopaminergic neuronal cells were exposed to 40 μM vanadium for 4.5 and 9 h and the intracellular Mn and Cu content of the cells was measured using the ICP-MS technique. Data represent results from three individual measurements and are expressed as mean ± S.E.M. *p<0.05, **p<0.01 and ***p<0.001.

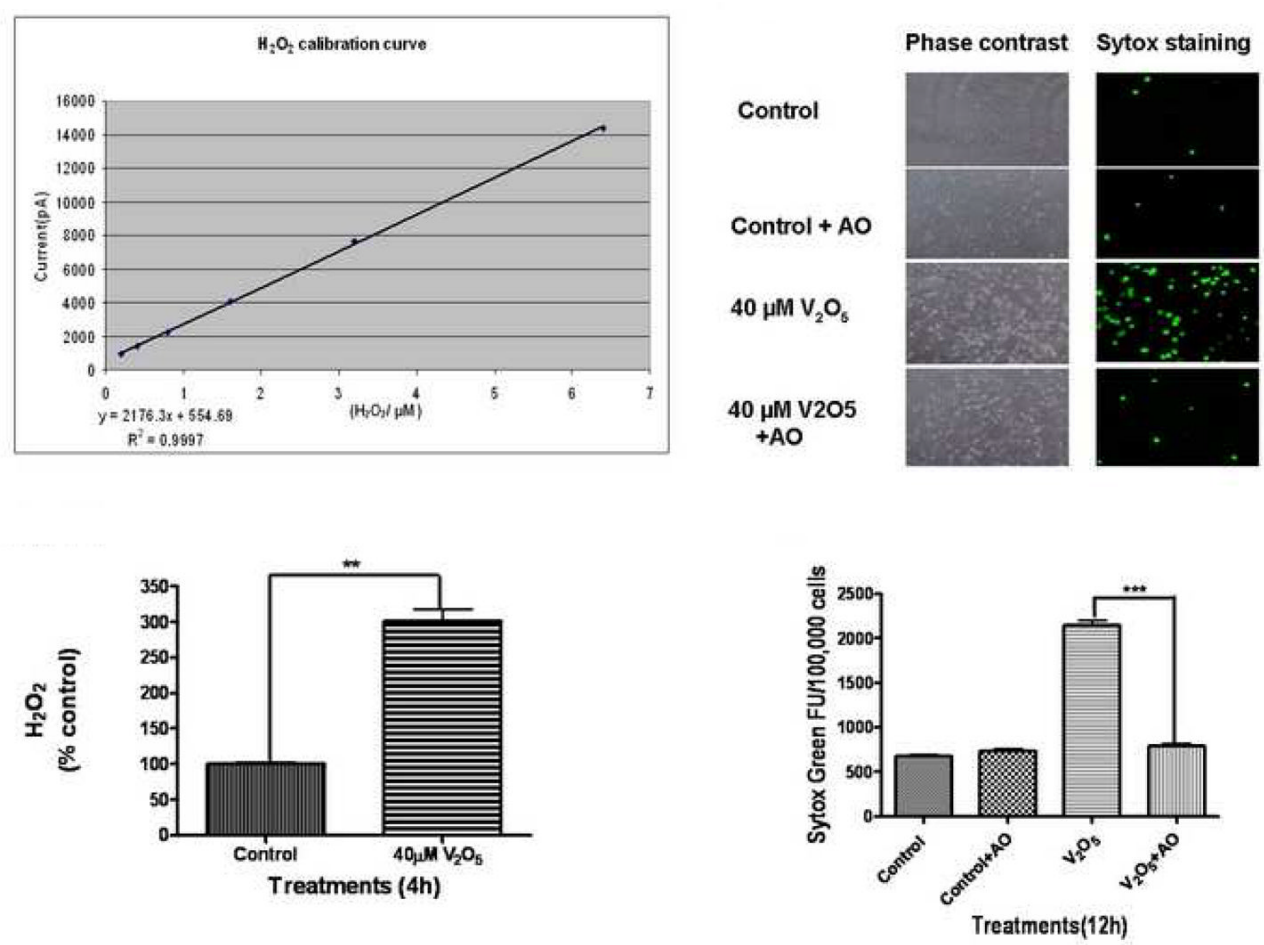

Fig. 3.

Role of oxidative stress in vanadium-induced neurotoxicity in N27 dopaminergic neuronal cells. **(A)** Calibration curve of H_2O_2 production by polarography: H_2O_2 production was measured using an Apollo 4000 Free Radical Analyzer (WPI, Sarasota, FL) equipped with a 100-µm H_2O_2 sensor. The 100-µm H_2O_2 sensor probe was calibrated using various doses of H_2O_2 according to the manufacturer's instructions. The calibration curve was used to calculate the H_2O_2 in the control and treatment groups. (**B)** Vanadium induced H_2O_2 generation in N27 cells. The measurements were conducted in a 96 well plate containing N27 cells exposed to 40 µM vanadium for 4 h. Each measurement was started by insertion of the 100-µm H_2O_2 sensor probe into wells containing cells. The output signal was recorded and compared to the standard curve. (**C)** Effect of antioxidants on vanadium-induced neurotoxicity. N27 dopaminergic neuronal cells were co-treated with vanadium and an antioxidant solution cocktail (AO) of vitamin E, glutathione, superoxide dismutase, and catalase. The Sytox green was added to cells and then cells were observed under a Nikon inverted fluorescence microscope. The pictures were captured with a SPOT digital camera (Diagnostic Instruments, Sterling Heights, MI). (**D)** Quantitative analysis of the protective effect of AO on vanadium-induced neurotoxicity was measured by the Sytox green cytotoxicity fluorescence assay. Data represent results from four individual measurements and are expressed as mean ± S.E.M. **p<0.001 and ***p<0.01.

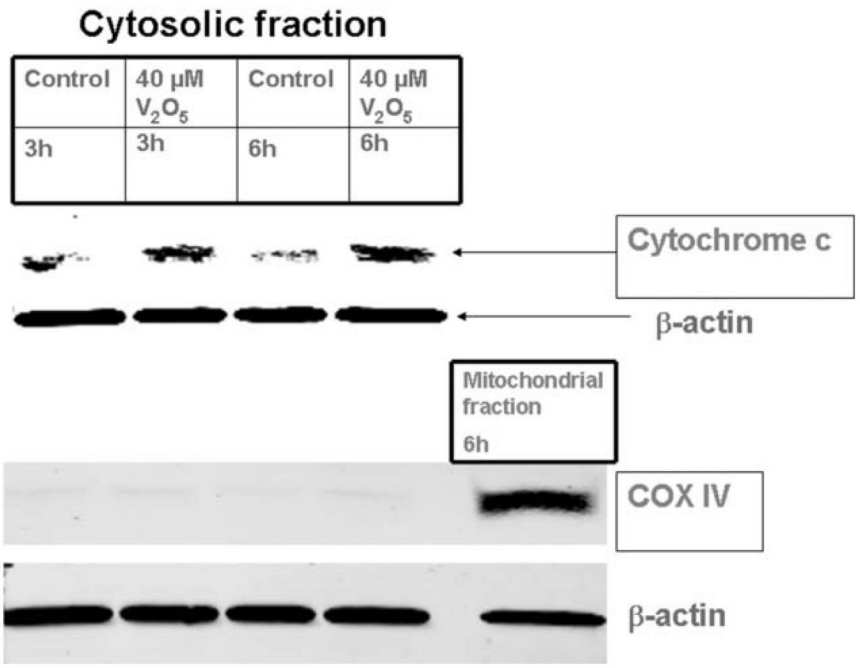

Fig. 4.

Mitochondrial release of cytochrome c in vanadium-treated N27 dopaminergic neuronal cells. The cells were treated with 40 μM vanadium for 3 and 6 h, cytosolic fractions were isolated, and cytochrome c was measured by Western blot. To confirm equal protein loading in each lane, the membranes were reprobed with β-actin antibody. The membranes were reprobed with COX-IV antibody to ensure purity of the cytosolic fraction and the mitochondrial fraction was used as a positive control. Data represent results from at least two separate measurements.

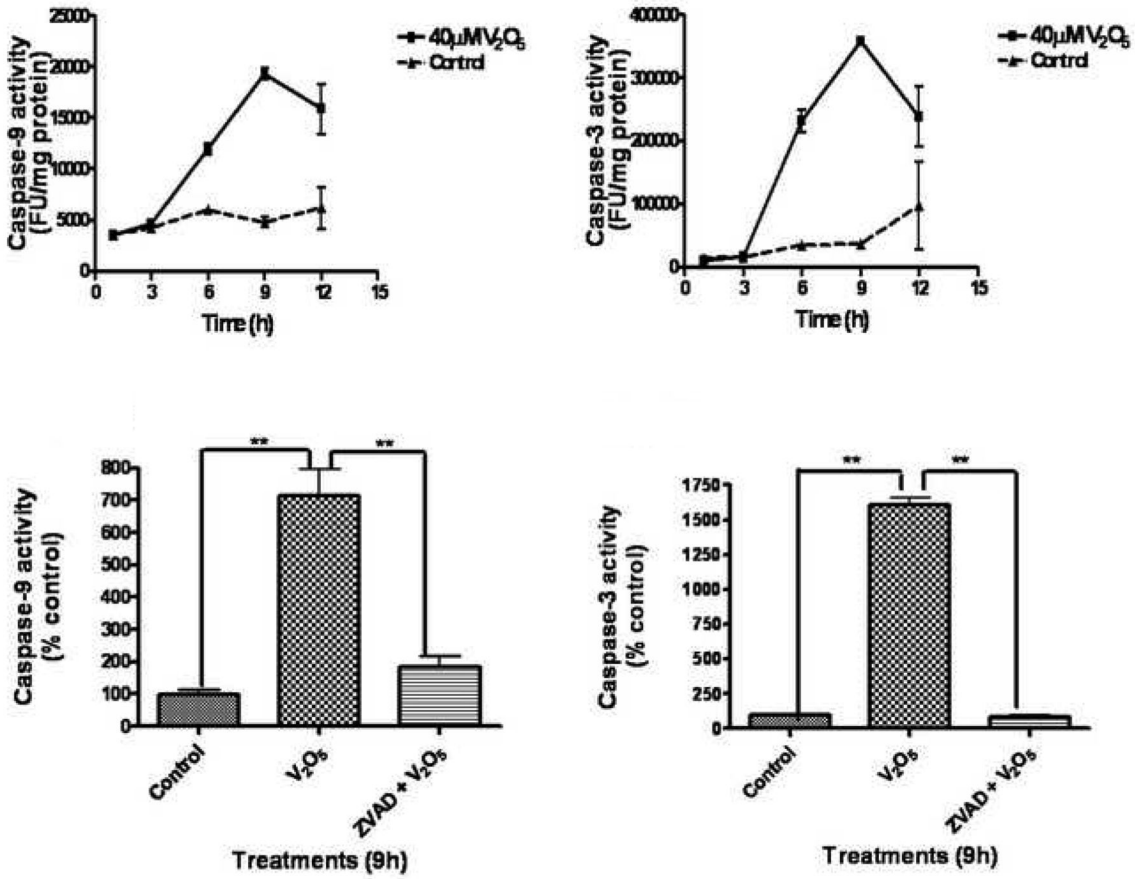

Fig. 5.

Activation of caspases-9 and -3 in vanadium-treated N27 cells. N27 dopaminergic cells were treated with 40 μM vanadium for 3, 6, 9 and 12 h. Caspase-9 **(A)** and caspase-3 **(B)** enzyme activities were assayed using caspase-9 and caspase-3 substrates, respectively. Effect of Z-VAD-FMK on caspase-9 **(C)** and caspase-3 **(D)** was tested following co-treatment with vanadium and the caspase inhibitor for 9 h. Data represent results from at least six individual measurements and are expressed as mean ± S.E.M. **p<0.01.

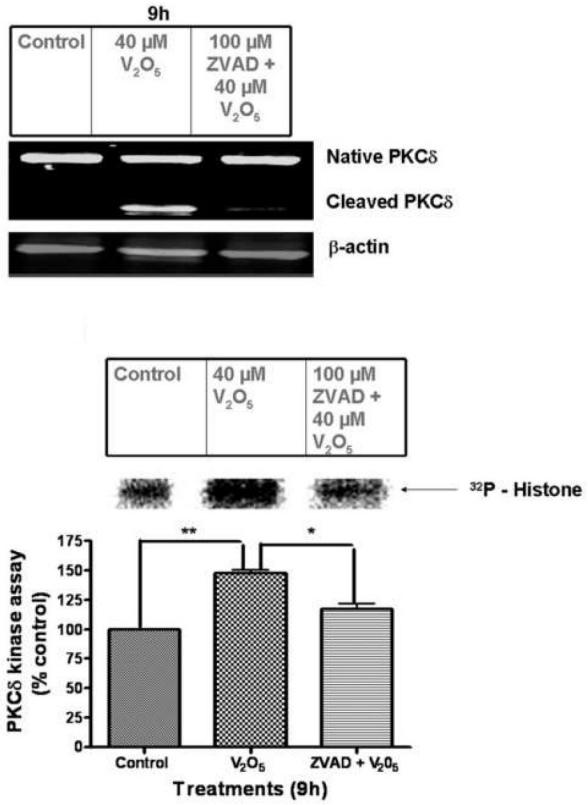

Fig. 6.

Caspase-dependent proteolytic cleavage of PKCδ in vanadium-induced neurotoxicity. **(A)** Vanadium-induced caspase-mediated PKCδ cleavage. PKCδ was immunoblotted after 40 μM vanadium treatment in N27 dopaminergic neuronal cells with or without the addition of 100 μM Z-VAD-FMK for 9 h. Proteins were separated from lysates by 12% SDS-PAGE and the immunoblot was probed with PKCδ antibody to observe both native (72–74 kDa) and cleaved (38–41 kDa) PKCδ bands. To confirm equal protein loading in each lane, the membranes were reprobed with β-actin antibody. Data represent results from at least two individual measurements. (**B)** Vanadium-induced PKCδ cleavage increases the kinase activity. N27 dopaminergic cells were harvested 9 h after treatment with 40 μM vanadium in the presence or absence of 100 μM Z-VAD-FMK. Cell lysates were isolated and PKCδ was immunoprecipitated from treated cell lysates and the enzyme activity was measured by ^{32}P phosphorylation. The values are expressed as a percentage of untreated control cells. Data represent results from at least three individual measurements and are expressed as mean ± S.E.M. *$p<0.05$ and **$p<0.01$.

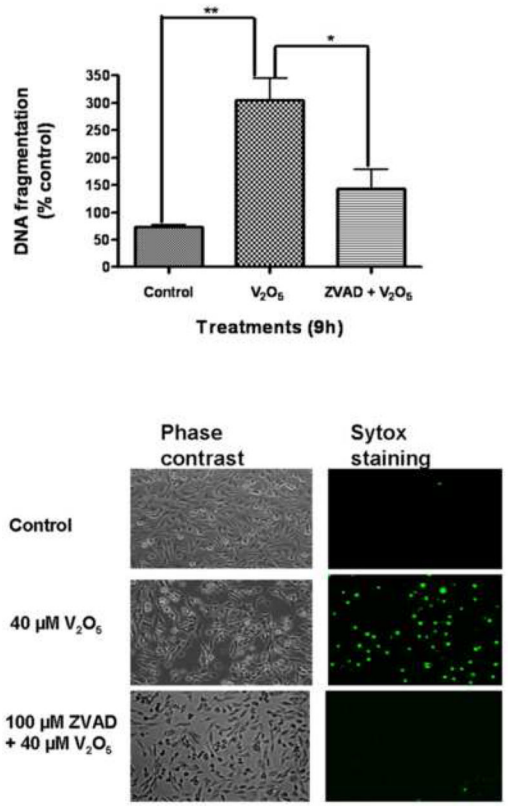

Fig. 7.

(A) Effect of Z-VAD-FMK on vanadium-induced DNA fragmentation in N27 dopaminergic neuronal cells. N27 cells were harvested 9 h after treatment with 40 μM vanadium in the presence or absence of 100 μM Z-VAD-FMK. DNA fragmentation was quantified using ELISA. The data are expressed as percentage of DNA fragmentation compared to untreated control cells. Data represent results from three individual measurements and are expressed as mean ± S.E.M. *$p<0.05$ and **$p<0.01$. **(B)** Visualization of the protective effect of the pan-caspase inhibitor Z-VAD-FMK on vanadium-induced cytotoxicity. Data represent results from three individual measurements. Sytox green positive cells were observed under a Nikon inverted fluorescence microscope and pictures were captured with a SPOT digital camera (Diagnostic Instruments, Sterling Heights, MI).

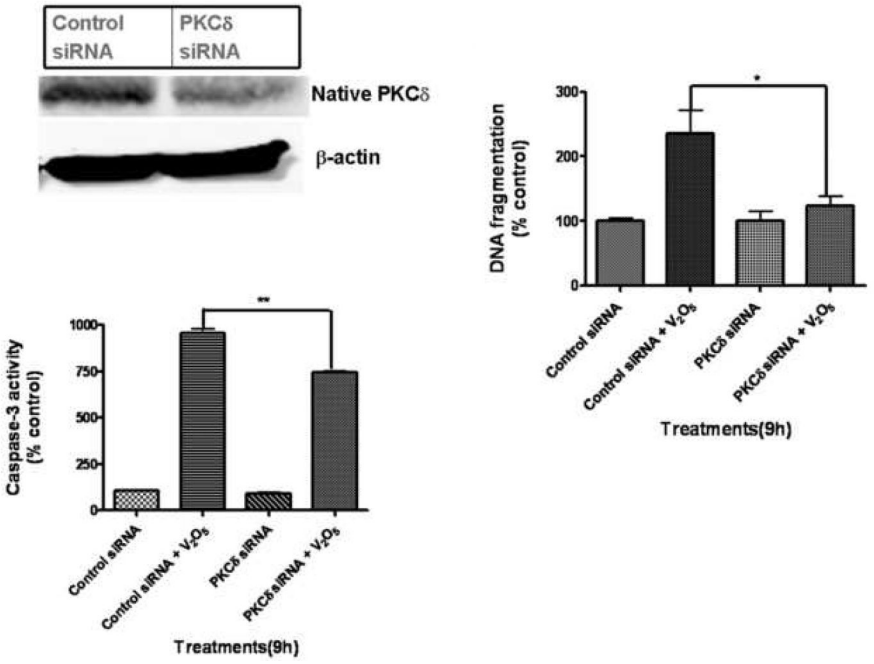

Fig. 8.

Effect of PKCδ knockdown by PKCδ-siRNA on vanadium-induced neurotoxicity. **(A)** PKCδ-siRNA suppresses PKCδ protein expression. N27 cells were transfected with PKCδ-siRNA (25 nM) or non-specific (NS)-siRNA for 24 h and PKCδ expression was determined by Western blotting. Membranes were reprobed with β-actin (43 kDa) antibody to confirm equal protein loading. Effect of PKCδ knockdown on vanadium-induced caspase-3 activity **(B)** and DNA fragmentation **(C)**. siRNA transfected N27 cells were exposed to 40 μM V_2O_5 for 9 h. Caspase-3 activity and DNA fragmentation were measured as described in the Methods. Data represent results from three individual measurements and are expressed as mean ± S.E.M. *p<0.05 and **p<0.01.

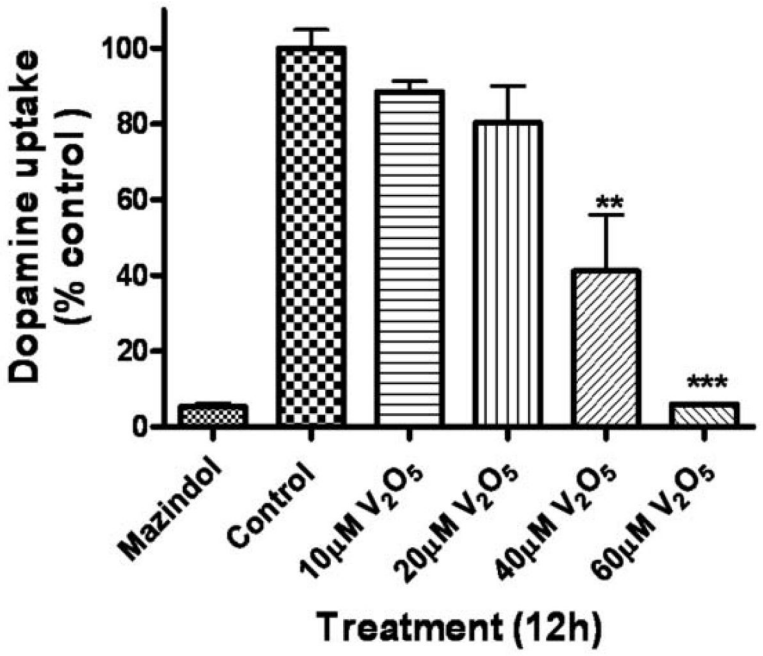

Fig. 9.

Neurotoxic effect of vanadium on primary nigral dopaminergic neurons. Mouse primary mesencephalic cultures were exposed to 10, 20, 40 and 60 μM vanadium for 12 h and the viability of dopaminergic neurons was measured by ^{3}H-DA uptake assay. Data represent results from two to six individual measurements and are expressed as mean ± S.E.M. **p<0.01 and ***p<0.001.

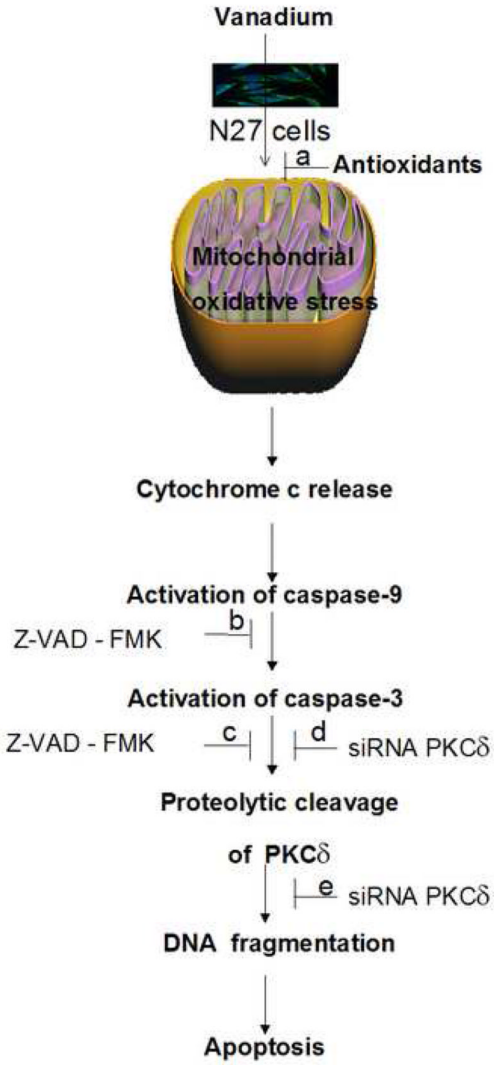

Fig. 10.

A model describing the sequence of cell death signaling events in vanadium-induced apoptosis. Vanadium treatment impairs mitochondrial function with an increase in ROS generation, resulting in cytochrome c release into the cytosol; cytosolic cytochrome c activates the caspase cascade; caspase-3 mediates proteolytic cleavage of PKCδ; proteolytically activated PKCδ mediates DNA fragmentation and apoptosis. Effect of pharmacological inhibitors and genetic modulators on vanadium-induced apoptosis: a, co-treatment with antioxidants prevents cell death; b and c, co-treatment with the pan-caspase inhibitor Z-VAD-FMK prevents proteolytic activation of PKCδ and vanadium-induced DNA fragmentation; d and e, RNAi-mediated knockdown of PKCδ with siRNA- PKCδ rescues N27 cells from vanadium-induced apoptotic cell death.